AD A046108

AFFDL-TR-76-162

12
B.S.

AN EXPOSITION ON AIRCRAFT RESPONSE TO ATMOSPHERIC TURBULENCE USING POWER SPECTRAL DENSITY ANALYSIS TECHNIQUES

Structural Integrity Branch
Structural Mechanics Division

DDC
RECEIVED
NOV 7 1977
F

May 1977

TECHNICAL REPORT AFFDL-TR-76-162

Final Report for Period October 1975 - August 1976

AD No.
DDC FILE COPY

Approved for public release; distribution unlimited

AIR FORCE FLIGHT DYNAMICS LABORATORY
AIR FORCE WRIGHT AERONAUTICAL LABORATORIES
AIR FORCE SYSTEMS COMMAND
WRIGHT-PATTERSON AIR FORCE BASE, OHIO 45433

NOTICE

When Government drawings, specifications, or other data are used for any purpose other than in connection with a definitely related Government procurement operation, the United States Government thereby incurs no responsibility nor any obligation whatsoever; and the fact that the government may have formulated, furnished, or in any way supplied the said drawings, specifications, or other data, is not to be regarded by implication or otherwise as in any manner licensing the holder or any other person or corporation, or conveying any rights or permission to manufacture, use, or sell any patented invention that may in any way be related thereto.

This report has been reviewed by the Information Office (ASD/OIP) and is releasable to the National Technical Information Service (NTIS). At NTIS, it will be releasable to the general public, including foreign nations.

This technical report has been reviewed and is approved for publication.

Elijah W Turner

ELIJAH W. TURNER
Project Engineer

R.M. Bader

ROBERT M. BADER, Chief
Structural Integrity Branch
Structural Mechanics Division

FOR THE COMMANDER

Howard L. Farmer

HOWARD L. FARMER, Col., USAF
Chief, Structural Mechanics Div.

DISTRIBUTION/AVAILABILITY CODES
SPECIAL
A

Copies of this report should not be returned unless return is required by security considerations, contractual obligations, or notice on a specific document.

AIR FORCE/56780/17 October 1977 — 250

UNCLASSIFIED

SECURITY CLASSIFICATION OF THIS PAGE (When Data Entered)

REPORT DOCUMENTATION PAGE

READ INSTRUCTIONS BEFORE COMPLETING FORM

1. REPORT NUMBER: AFFDL-TR-76-162

2. GOVT ACCESSION NO.

3. RECIPIENT'S CATALOG NUMBER

4. TITLE (and Subtitle): AN EXPOSITION ON AIRCRAFT RESPONSE TO ATMOSPHERIC TURBULENCE USING POWER SPECTRAL DENSITY ANALYSIS TECHNIQUES

5. TYPE OF REPORT & PERIOD COVERED: Final Technical Report. Oct 75 - Aug 76

6. PERFORMING ORG. REPORT NUMBER

7. AUTHOR(s): Elijah W. Turner

8. CONTRACT OR GRANT NUMBER(s)

9. PERFORMING ORGANIZATION NAME AND ADDRESS: Air Force Flight Dynamics Laboratory/FBE, Air Force Systems Command, Wright-Patterson AFB, Ohio 45433

10. PROGRAM ELEMENT, PROJECT, TASK AREA & WORK UNIT NUMBERS: 13670113 01

11. CONTROLLING OFFICE NAME AND ADDRESS: Air Force Flight Dynamics Laboratory/FBE, Air Force Systems Command, Wright-Patterson AFB, Ohio 45433

12. REPORT DATE: May 1977

13. NUMBER OF PAGES: 73

14. MONITORING AGENCY NAME & ADDRESS (if different from Controlling Office): 73p.

15. SECURITY CLASS. (of this report): Unclassified

15a. DECLASSIFICATION/DOWNGRADING SCHEDULE

16. DISTRIBUTION STATEMENT (of this Report)

Approved for public release; distribution unlimited.

17. DISTRIBUTION STATEMENT (of the abstract entered in Block 20, if different from Report)

DDC
NOV 7 1977
F

18. SUPPLEMENTARY NOTES

19. KEY WORDS (Continue on reverse side if necessary and identify by block number)

Aircraft Response
Power Spectral Density
Atmospheric Turbulence

20. ABSTRACT (Continue on reverse side if necessary and identify by block number)

The traditional power spectral density design procedure is reviewed. The evolution of modeling atmospheric turbulence is traced from the discrete gust to the present continuous representation. The modeling of an aircraft structure as a lumped parameter linear system excited by oscillatory air forces is outlined, and solutions to the resulting equations of motion are indicated.

Expressions for the number of exceedances of specified load levels are presented and compared for stationary Gaussian turbulence and for stationary

DD FORM 1 JAN 73 1473 EDITION OF 1 NOV 65 IS OBSOLETE

UNCLASSIFIED

SECURITY CLASSIFICATION OF THIS PAGE (When Data Entered)

012 070

1B

Abstract Continued --

Gaussian patch turbulence.

The motivation for modeling atmospheric turbulence as a nonstationary process is addressed, and several models for nonstationary turbulence are reviewed.

FOREWORD

This report was prepared by E. W. Turner, Aerospace Engineer in the Loads and Response Prediction Group of the Structural Mechanics Division of the Air Force Flight Dynamics Laboratory at Wright-Patterson Air Force Base, Ohio. The work described herein is a part of the Air Force Systems Command exploratory development program to predict aircraft response to atmospheric turbulence. The work was directed under Project 1367, "Structural Integrity for Military Aerospace Vehicles," Task 136701, "Structural Flight Loads Data."

This report covers work done in the period from October 1975 to August 1976. This manuscript was released by the author in September 1976 for publication as an AFFDL Technical Report.

ACCESSION for
NTIS White Section
DDC Buff Section
UNANNOUNCED
JUSTIFICATION
BY
DISTRIBUTION/AVAILABILITY CODES
A

TABLE OF CONTENTS

Section	Title	Page
I	INTRODUCTION	1
II	ATMOSPHERIC TURBULENCE MODELS	3
	1. Discrete Gusts	3
	2. Continuous Turbulence Models	6
	3. Power Spectra	7
III	DYNAMIC ANALYSIS	18
	1. Overview	18
	2. Lumped Parameter System	19
	3. Mass and Stiffness Matrices	20
	4. Normal Modes	20
	5. Equations of Motion	21
	6. Load Equations	23
	7. Aerodynamic Forces	24
	8. Aerodynamic Theories	26
	9. Solution to the Equations of Motion	27
	10. Solution to the Load Equations	29
IV	SPECTRAL ANALYSIS	31
	1. Design Envelope Analysis	33
	2. Mission Analysis	35
V	NONSTATIONARY TURBULENCE MODELS	39
	1. Transient Overloads	41
	2. Uniformly Modulated Process	42
	3. Time Varying Power Spectra	43
	4. Self-Similarity	45
VI	CONCLUSIONS	48
	APPENDIX A -- DERIVATION OF EXCEEDANCE EQUATION	49
	APPENDIX B -- SELF-SIMILARITY RELATION FOR VON KARMAN SPECTRA	57
	REFERENCES	59

Preceding Page Blank - NOT FILMED

LIST OF ILLUSTRATIONS

Figure	Title	Page
1.	PSD Design Procedure	2
2.	Derived Gust Velocity for Gust Loads Formula	5
3.	Sample Time Histories of Vertical Gust Velocity	8
4.	Typical Power Spectra of Vertical Gust Velocity	11
5.	Variety of Power Spectra of Vertical Gust Velocity Measured in Cumulus Clouds	12
6.	Measured and Fitted von Karman Spectra of Vertical Gust Velocity from Severe Storm	15
7.	RMS Gust Velocity of Storm and Non-Storm Turbulence	16
8.	Probability of Encountering Storm and Non-Storm Turbulence	17
9	Frequency Response Function of Simple Damped Oscillator	28
10.	Frequency Response Function of First Free-Free Airplane Mode of Vibration	30
11.	Frequency Response Function of Wind Bending Moment at 1/3 Span	30
12.	Derived Gust Velocity for Design Envelope Analysis	34
13.	Mission Profile of Training Mission	37
14.	Typical Exceedance Curve	37
15.	Gaussian Exceedance Curve	39
16.	Gaussian-Patch Exceedance Curve	40
17.	Modulating Function	41
18.	Nonstationary Excitation Function	42
19.	Procedure to Determine Effects of Nonstationary Excitation of the Spectra of Atmospheric Turbulence	46
20.	Typical Response Time History	49
21.	Typical Level Crossing	50

LIST OF SYMBOLS

$\bar{A}$	Ratio of rms response to rms excitation
$[A]$	Matrix of oscillatory panel forces per unit sinusoidal panel displacement
$[A_g]$	Matrix of oscillatory panel forces per unit sinusoidal angle of attack
$A(t,\omega)$	Time varying transfer function
a_z	Vertical acceleration of aircraft
$a(t)$	Deterministic modulating function
b_i	rms gust velocity of turbulence of type i
$\bar{c}$	Mean aerodynamic chord
$C_{L\alpha}$	Aircraft lift curve slope
$\{c\}$	Matrix of modal forces due to unit sinusoidal gust velocity
$\{c_o\}$	Matrix of maximum values of c
$\{C_R\}$	Matrix of maximum values of c for load equations
$[D]$	Generalized damping matrix
$[D_A]$	Generalized aerodynamic damping matrix
$[D_R]$	Generalized damping matrix for response load equations
$[D_S]$	Generalized structural damping matrix
e	Base of natural logarithms, 2.71828...
$f(t)$	Modulating function of "uniformly modulated" process
$F(h)$	Relation between wavelength and amplitude of self-similar process
$[G]$	Transformation matrix from 2-D panel forces to 3-D panel forces
$[g]$	Damping coefficient matrix

LIST OF SYMBOLS (CONTINUED)

g	Acceleration of gravity
$g(t)$	Gaussian random process
$H(\omega)$	Transfer function
i	$\sqrt{-1}$
$[K]$	Generalized stiffness matrix
$[K_A]$	Generalized aerodynamic stiffness matrix
$[K_R]$	Generalized stiffness for response load equations
$[K_S]$	Generalized structural stiffness matrix
$[K_f]$	Stiffness matrix
κ_w	Gust alleviation factor
L	Scale of turbulence
l_x	Distance from gust vane to aircraft center of gravity
m_i	Mass of the ith lumped mass point
$[M]$	Generalized mass matrix
$[M_A]$	Generalized aerodynamic mass matrix
$[M_R]$	Generalized mass for response load equations
$[M_S]$	Generalized structural mass matrix
$[M_f]$	Mass matrix
n	Load factor in turbulence
n_o	Load factor in steady level flight
$N(y)$	Number of exceedances of level y per unit time
N_o	Number of exceedances of level $y = 0$ per unit time
$p(x)$	Probability density function

LIST OF SYMBOLS (CONTINUED)

$p(y,\dot{y})$	Joint probability density function
P_i	Probability of encountering turbulence of type i
q	Dynamic pressure
$\{q\}$	Matrix of deflections of the generalized coordinates
$\{q_o\}$	Matrix of maximum values of [g]
$\{Q_R\}$	Matrix of generalized modal forces due to modal deflections
$\{R\}$	Matrix of the response of the load equations
$R(\tau)$	Autocorrelation function
$R_w(\tau)$	Autocorrelation function of atmospheric turbulence
$R_{o_z}(\tau)$	Autocorrelation function of a Gaussian process whose zero crossings are identical to those of Z(t)
S	Wing area
T	Duration of composite mission
T_i	Duration of ith mission segment
t_i	Ratio of duration of ith mission segment to duration of total mission
t	Time
U_e	Equivalent velocity of 25 $\bar{c}$ one-minus-cosine gust
U_{de}	Equivalent derived velocity of 25 $\bar{c}$ one-minus cosine gust
U_σ	Nominal rms turbulence intensity for design
V_T	True velocity
V_e	Equivalent velocity
V_{KEAS}	Equivalent air speed in knots
V_L	Limit velocity in landing configuration
V_H	Maximum continuous velocity in level flight

LIST OF SYMBOLS (CONTINUED)

V_C	Maximum cruise velocity
V_G	Velocity for gust penetration
V_D	Maximum dive velocity
v_g	True lateral gust velocity
W	Gross weight
w(t)	Random process model of turbulence
$w_g(t)$	True vertical gust velocity
w_g	Maximum value of $w_g(t)$
X(t)	Random process
$X(t,\omega,\Delta\omega)$	Component of X(t) within frequency band $\omega \pm \frac{\Delta\omega}{2}$
$\{X\}$	Matrix of structural deflections
y	Design parameter
y_{DESIGN}	Value of y used in design
y_{LA}	Limit allowable value of y
y_{1-g}	Value of y in steady, level 1-g flight
z(t)	Gaussian random process
α_v	Angle of attack of gust vane
$\alpha_g(t)$	Angle of attack induced by gust velocity
β	Ramp function severity factor
ζ	Ratio of actual damping to critical damping
η_d	Ratio of "correct" design value to rms design value
θ	Pitch angle of attack
Θ	Phase angle delay of panel excitation

LIST OF SYMBOLS (CONTINUED)

λ	Panel location aft of reference point
μ	Aircraft mass ratio, $\frac{2W/S}{g\bar{c}C_{\ell\alpha}\rho}$
μ_x	Mean value of X
π	3.14159...
ρ	Density of air at flight altitude
ρ_o	Density of air at sea level
σ	RMS intensity of gust patch
σ_x^2	Variance of X(t), mean square value
σ_w	RMS gust intensity over all patches of turbulence
τ	Time delay for correlation, $t_2 - t_1$
ϕ_{ij}	Deflection at the ith lumped mass point due to unit deflection of the jth generalized coordinate
$\phi(\Omega)$	Power spectral density function
$\phi(t,\Omega)$	Evolutionary power spectral density function
$\phi(\Omega,t)$	Instantaneous power spectral density function
$[\phi]$	Transformation matrix from displacements in the generalized coordinate system to deflections at the aerodynamic panels
ϕ	Phase angle between excitation and response
Ω	Spacial frequency, ω/V_T
ω	Frequency in radians per unit time
ω_c	"Cut-off" frequency
ω_{Ni}	Frequency of ith normal mode
$[\quad]$	Rectangular matrix
$\{\quad\}$	Column matrix
$\cdot$	Derivative with respect to time

LIST OF SYMBOLS (CONTINUED)

$[\quad]^T$ Transpose of a matrix

$[\quad]^{-1}$ Inverse of a matrix

SECTION I
INTRODUCTION

The traditional Power Spectral Density (PSD) analysis for calculating the response of an aircraft to continuous turbulence has evolved through a continual effort to account more precisely for the unpredictable nature of turbulence. Although few will question that the PSD analysis does a considerably better job of representing the true nature of turbulence than the discrete gust model, the traditional PSD analysis has been questioned because it under predicts the presence of turbulence in the higher intensities.

This report is an effort to view the traditional PSD analysis and the reported deficiences in their proper perspective. Hence the entire approach, depicted in Figure 1, and the basic assumptions are reviewed. The deficiencies are then discussed, and finally, the most recent efforts to characterize turbulence are presented.

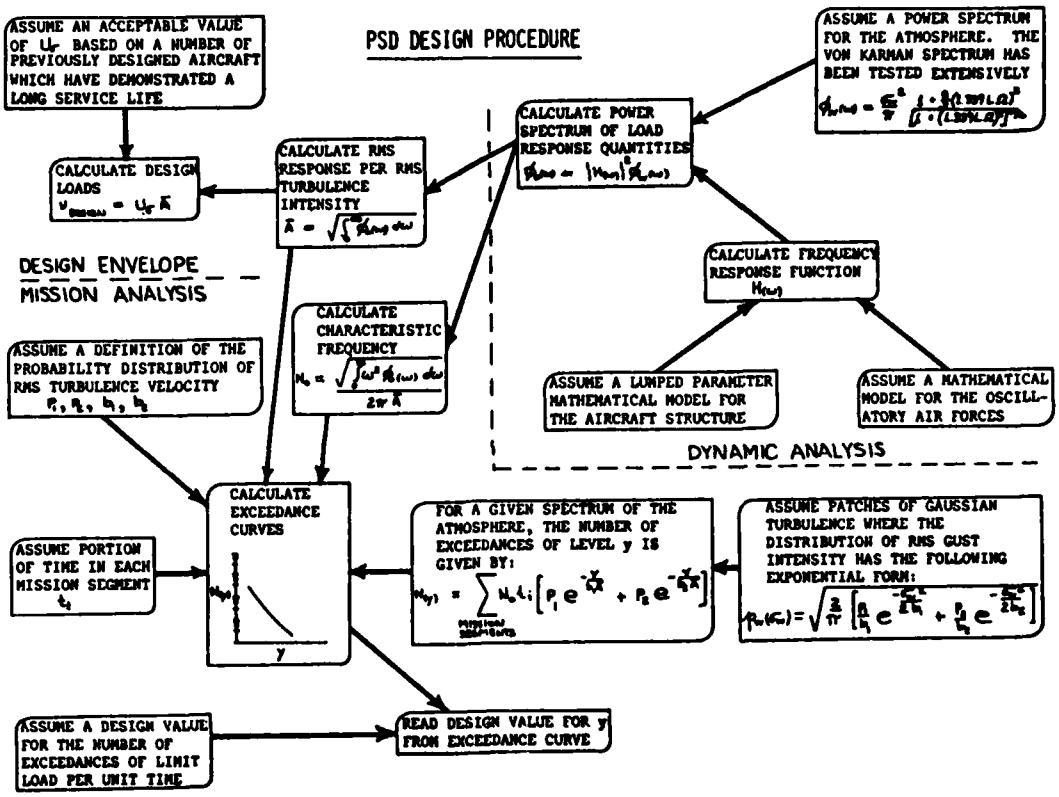

Figure 1. PSD Design Procedure

SECTION II

ATMOSPHERIC TURBULENCE MODELS

One day after a particularly rough flight in gusty winds, Wilbur supposedly remarked to Orville, "Once we get above the trees, we won't have to worry about this bumpiness." Similarly, the prevailing thought until not too long ago was that flights above the clouds would be in still air. The discovery of the jet stream, temperature inversions, mountain waves, and other types of turbulence proved these theories to be false.

Above the region in which the atmosphere behaves as a boundary layer, the numerous types of turbulence are frequently divided into two categories: (1) convective turbulence in and around clouds, particularly thunderstorms, and (2) CAT, which is an acronym for Clear Air Turbulence. Below the cloud bases, surface heating may result in direct buoyant convection and many small eddies that are perceived as mild CAT. Above a field of cumulus clouds, a regular "chop" may persist where there is significant gradients in the wind velocity with altitude. Some of the more violent types of CAT are associated with mountain and lee waves which may have rotors (vortices) embedded in them at regular intervals. Flights in the vicinity of the jet stream and near the tropopause can be particularly turbulent, depending on meteorological conditions. Some of the most violent turbulence of all exists in thunderstorms and squall lines, particularly in areas of heavy precipitation. The mechanism (Reference 1) for generating this turbulence is convection which produces rising and falling columns of air ringed by toroids of extreme vorticity. The mechanism of turbulence is such a varied and complicated process that statistics offer the only manageable method to handle the gust design problem.

1. DISCRETE GUSTS

For the purpose of design for gust encounter, a description (or model) of atmospheric turbulence is required. For simplicity, an analytical model is desirable. Early models characterized turbulence as a discrete

gust and the "sharp edged gust" is of this type. Neglecting lift growth, the maximum response of a rigid aircraft to a sharp edged gust is:

$$n = n_o + \frac{q S C_{\ell\alpha} U_e}{W V_e} = n_o + \frac{\rho_o V_e C_{\ell\alpha} U_e}{2W/S} \qquad (1)$$

where:

n_o = load factor in steady level flight = 1.0
n = load factor in turbulence
q = dynamic pressure = $\frac{1}{2}\rho_o V_e^2$, lbs/ft^2
S = wing area, ft^2
$C_{\ell\alpha}$ = lift curve slope
W = gross weight, lbs
V_e = airspeed (equivalent), ft/sec
U_e = gust velocity (equivalent), ft/sec
ρ_o = air density at sea level, lb sec^2/ft^4

This model evolved into a "one-minus-cosine" gust in an effort to use a more realistic waveform. The factor K_w was added to account for this waveform and also to account for the finite length of time required for lift to develop the following gust encounter, which is referred to as "lift growth."

$$n = n_o + \frac{\rho_o V_e C_{\ell\alpha} U_{de} K_w}{2W/S} \qquad (2)$$

By substituting $V_{keas} = 1.689\ V_e$ and $\rho_o = .002377$, this equation becomes the so-called "gust loads formula" which has been used in design extensively.

$$n = n_o + \frac{V_{KEAS} C_{\ell\alpha} U_{de} K_w}{498\ W/S} \qquad (3)$$

where:

$$498 = \frac{2.0}{(1.689)\ (0.002377)} \qquad (4)$$

U_{de} = derived gust velocity, ft/sec

V_{keas} = knots equivalent airspeed

W/S = wing loading, lbs/ft^2

Values for the somewhat arbitrary factor K_w are given in terms of aircraft mass ratio μ for aircraft at subsonic airspeeds as:

$$K_w = \frac{0.88\mu}{5.3+\mu} \tag{5}$$

and for aircraft at supersonic airspeeds as:

$$K_w = \frac{\mu^{1.03}}{6.95+\mu^{1.03}} \tag{6}$$

where

$$\mu = \frac{2W/S}{g\,\bar{c}\,C_{\ell\alpha}\,\rho} \tag{7}$$

and

g = 32.2 ft/sec^2

$\bar{c}$ = mean aerodynamic chord, feet

ρ = air density at flight altitude, lb sec^2/ft^4

Design values of gust velocity for use in the gust loads formula were established following analysis of many hours of VGH (velocity-load factor-altitude) data. Essentially, the gust loads formula was solved in reverse for measured occurrences of load factor peaks, to determine what gust velocity from a 25-chord gust would produce the observed peak. Accepted design values for the derived gust velocity U_{de} are given in Figure 2. These values are specified in paragraph 25.341 of the Federal Aviation Regulations.

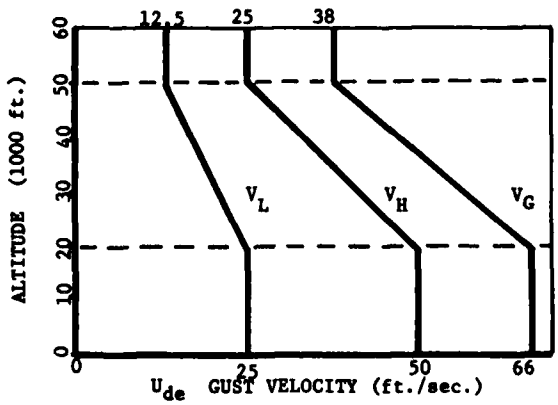

Figure 2. Derived Gust Velocity for Gust Loads Formula

where

V_L = limit speed for the basic high drag (landing) configuration

V_H = maximum continuous speed in level flight

V_G = gust penetration speed

2. CONTINUOUS TURBULENCE MODELS

The 25-chord wavelength for the one-minus-cosine gust was selected because this wavelength historically couples with the vertical translation and short-period pitch modes of the rigid airplane to produce the largest induced load factor. With the development of higher speed aircraft with increased flexibility, the possibility of other wavelengths coupling with flexible modes to produce significant response is increased. In an effort to consider all of the possible wavelengths, and the magnitude of the gust associated with those wavelengths, investigators turned to power spectral techniques for aircraft design. This analysis is based on a model which characterizes turbulence as a stationary random process; considerable time and effort was expended to collect sufficient data to establish this model.

As part of an Air Force sponsored "Critical Air Turbulence (CAT)" investigation, instruments were installed on fixed towers to record true gust velocities at low altitudes, and instrumented aircraft were flown to collect flight data under various meteorological conditions and altitudes. The data which must be collected in flight in order to calculate time histories of gust velocity consist of continuous recording of airflow direction, airspeed, and aircraft motions. Three axis airflow directions were recorded from flow vanes mounted on a boom on the nose of the test aircraft. The measured parameters which define the aircraft motion consist of three axis accelerations (a_x, a_y, a_z) and two axis rotation rates (pitch and yaw rates). These parameters are used in conjunction with the equations of motion of the aircraft to convert angle of attack of the boom mounted vanes to gust velocities and to remove the contributions from the aircraft

motion. The following equation illustrates this for the case of vertical gust velocity:

$$W_g = (\alpha_v - \theta) V_T + \ell_x \dot{\theta} + \int a_z \, dt \tag{8}$$

where

W_g = true vertical gust velocity

α_v = angle of attack of boom mounted vane

θ = pitch angle of attack

$\dot{\theta}$ = pitch rate of aircraft

V_T = true velocity of aircraft

l_x = distance from vane to center of gravity of aircraft

a_z = vertical acceleration of aircraft

All of the parameters are measured from the mean values taken over the complete record.

Although more precise equations are sometimes used, it is convenient to assume that the aircraft and boom are completely rigid, and that the angles involved in the calculations of gust velocities are small enough that the accuracy is not lost by assuming small-angle theory. Variations in upwash at the vane location on the boom are either neglected, or are accounted for in the calibration of the vanes. Some sample time histories of vertical and lateral gust velocity appear in Figure 3 (Reference 2).

3. POWER SPECTRA

The Power Spectral Density (PSD) of a time varying function X(t) is a real function which shows how the mean square value of X(t) is distributed with frequency. The ordinate of the PSD curve at a particular frequency, ω, is the mean square value of that part of X(t)

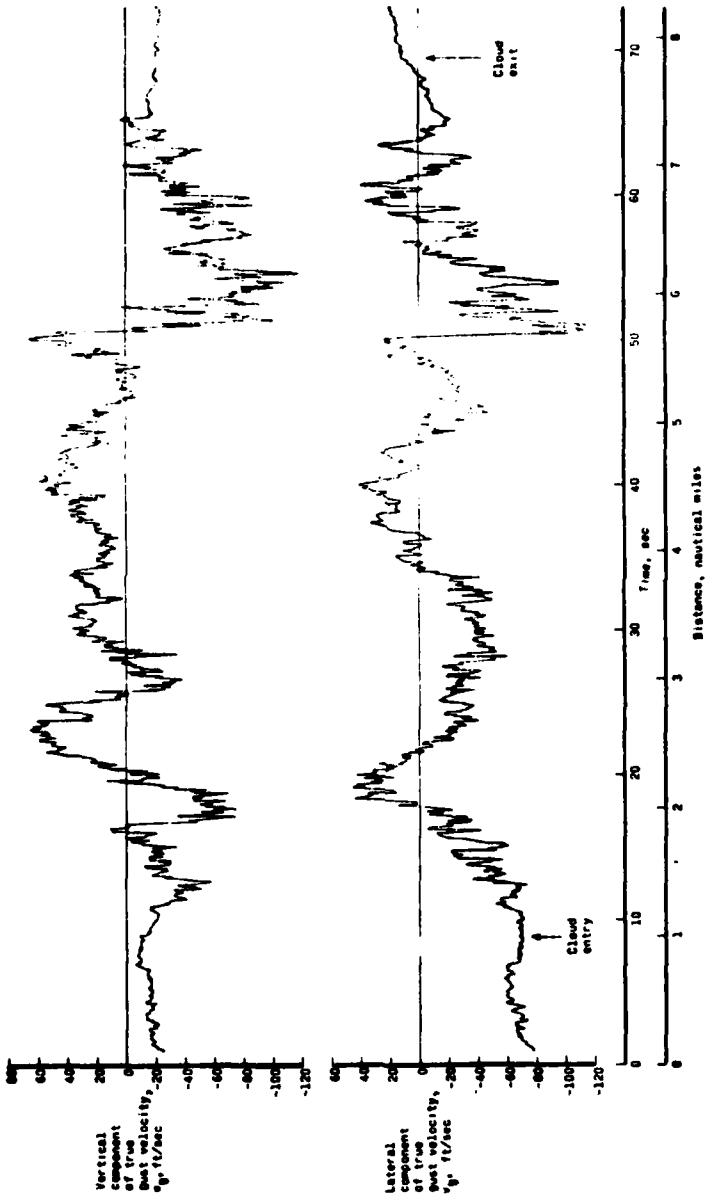

Figure 3. Sample Time Histories of Vertical Gust Velocity

whose frequency is within an infinitely narrow band centered about the frequency ω. This may be expressed as:

$$\phi(\omega) = \lim_{\substack{\Delta\omega \to 0 \\ T \to \infty}} \frac{1}{T\Delta\omega} \int_0^T X^2(t,\omega,\Delta\omega)\,dt \tag{9}$$

where

$\phi(\omega)$ = power spectral density function of $X(t)$ in units of $(ft/sec)^2/(rad/sec)$

T = duration of $X(t)$ in seconds

$X(t,\omega,\Delta\omega)$ = component of $X(t)$ within frequency band $\omega \pm \frac{\Delta\omega}{2}$

The total area under the PSD curve is the mean square value of $X(t)$ taken over all frequencies.

In order to remove the effects of variations in flight speed from one analysis to another, power spectra of the atmosphere are calculated on the basis of a spacial frequency defined as:

$$\Omega = \frac{\omega}{V_T} \tag{10}$$

where

Ω = spacial frequency in radians per foot

ω = circular frequency as observed by the aircraft in radians per second

V_T = true velocity of the aircraft in feet per second

The relation between the original and the transformed power spectra is given by:

$$\phi(\omega) = \frac{1}{V_T}\,\phi(\Omega) \tag{11}$$

Although it is possible to calculate the power spectra directly from the definition, it is more convenient to first calculate the autocorrelation function, $R(\tau)$, for the complete record, and then obtain the power spectrum, $\phi(\Omega)$, by performing a Fourier transform of the autocorrelation function using the Cooley-Tukey Fast Fourier Transform (FFT) technique.

$$R(\tau) = \frac{1}{T} \int_0^T X(t)\, X(t+\tau)\, dt \tag{12}$$

and

$$\phi(\Omega) = \frac{1}{2\pi} \int_{-\infty}^{\infty} R(\tau)\, e^{i\Omega\tau}\, d\tau \tag{13}$$

Typical power spectra of three different meteorological conditions are shown in Figure 4 (Reference 2). The height of the curve is a measure of the intensity of the turbulence at particular frequencies, and these show a characteristic decrease in intensity with increase in frequency. The square root of the area under the power spectra curve is a measure of the overall rms gust velocity, σ. Since the power spectra, in theory, extends from zero frequency to infinite frequency, and in practice there is some maximum frequency which is considered called the cutoff frequency, ω_c, there are two possible values of σ. In practice, only the area under the measured power spectrum is included in the rms value, even though the total rms value, if all of the area were to be considered from zero to infinity, might be 2 to 2.5 times greater (Reference 3). However, the power in the higher frequencies contributes very little to the response of an aircraft.

Power spectra measured in cumulus clouds are shown in Figure 5, (Reference 2) indicating that all of a wide variety of rms values demonstrate the characteristic decrease in power with increasing frequency. Analysis of numerous spectra under varying meteorological conditions indicates that a composite of all possible spectra would result in a continuous band of intensities varying from near zero to possibly

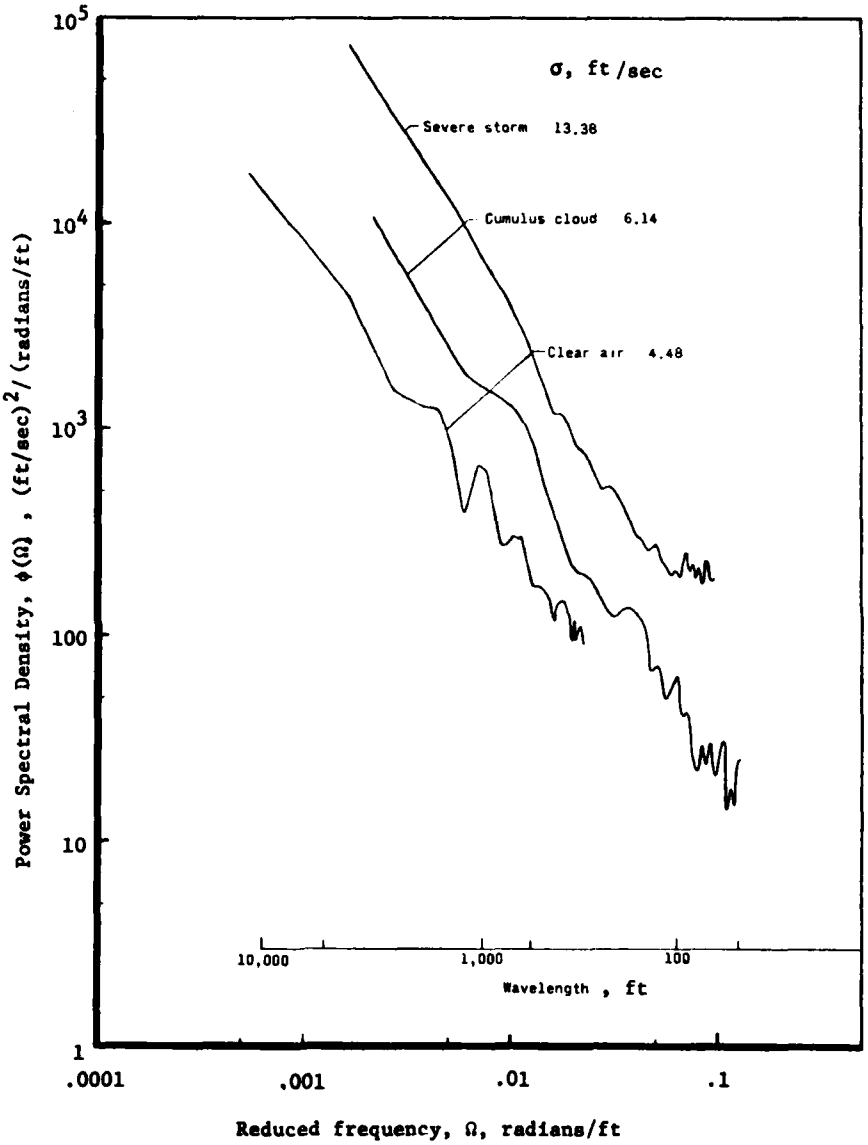

Figure 4. Typical Power Spectra of Vertical Gust Velocity

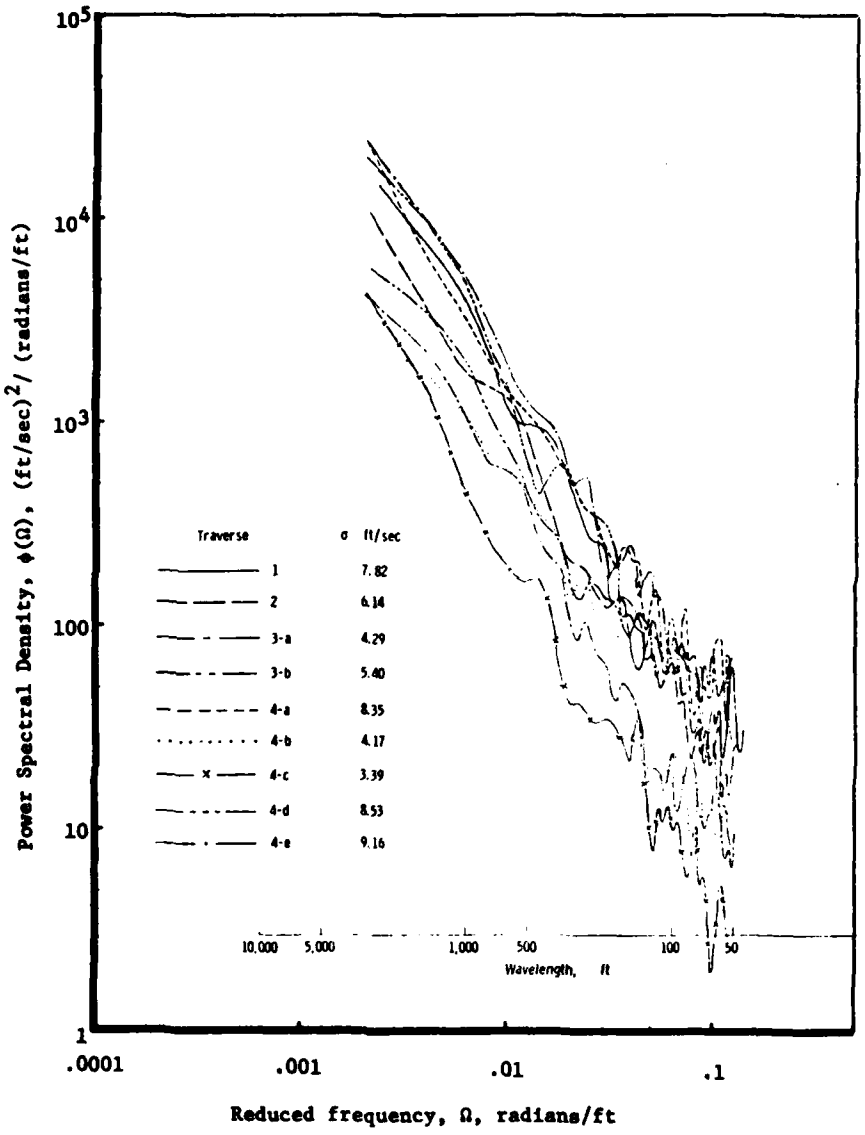

Figure 5. Variety of Power Spectra of Vertical Gust Velocity Measured in Cumulus Clouds

as high as 16 feet per second rms (Reference 2). Two analytical representations for the power spectrum of atmospheric turbulence have received extensive use. The "Dryden" spectrum

$$\phi(\Omega) = \frac{\sigma^2 L}{\pi} \frac{1 + 3L^2\Omega^2}{(1 + L^2\Omega^2)^2} \tag{14}$$

L = Scale of Turbulence

Dryden Spectra

is the simplest of the two and was first used to define the turbulence spectra in wind tunnels. The von Karman spectra:

$$\phi(\Omega) = \frac{\sigma^2 L}{\pi} \frac{1 + \frac{8}{3}(1.339L\Omega)^2}{\left[1 + (1.339L\Omega)^2\right]^{11/6}} \tag{15}$$

von Karman Spectrum

is more complicated, but is a better fit to the recorded spectra for atmospheric turbulence.

Figure 6 (Reference 2) shows recorded spectra and spectra that have been fitted using the von Karman representation. The parameter L is called the "scale of turbulence" and is a measure of the average eddy size. More precisely, L is the horizontal separation in space at which the gust velocities no longer display any correlation. Considerable testing of the von Karman spectrum has established that it is a reasonable fit to all levels of turbulence and that the value of L appears to be a function of altitude. Observations indicate that the rms turbulence intensity, σ, of the two previously mentioned categories of turbulence also vary with altitude independent of each other. The first category is referred to as "non-storm" and the second category is referred to as "storm." In Figure 7 (Reference 4) b_1 is the rms turbulence intensity averaged over the time that the aircraft is in non-storm turbulence, and b_2 is the corresponding intensity for storm turbulence.

As indicated by b_2, storm turbulence is most severe at about 25,000 feet altitude and reaches an rms intensity level of almost 12 feet per second at that altitude. The probability of turbulence (fraction of flight time in turbulence), however, is greater at the lower altitudes. In Figure 8 (Reference 4) P_1 is the probability of non-storm turbulence at various altitudes and P_2 is the same result for storm turbulence. Especially in the higher altitudes, the greatest portion of a flight will be in smooth air as indicated by the fact that $P_1 + P_2 < 1$.

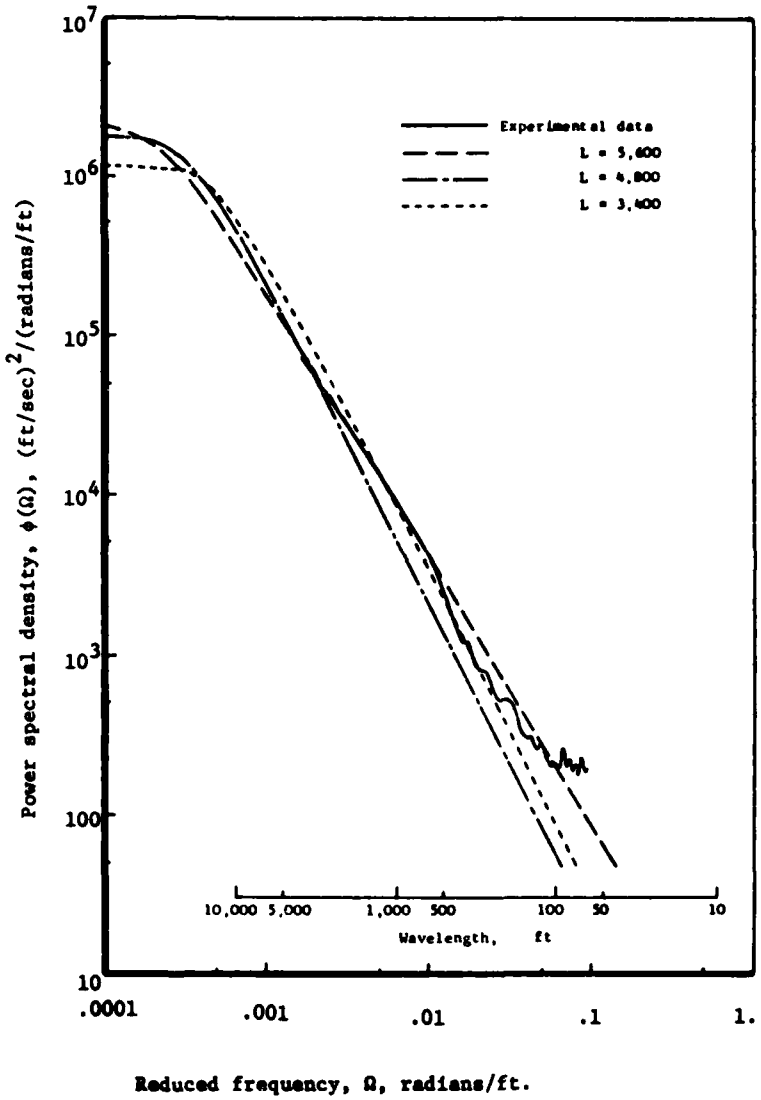

Figure 6. Measured and Fitted Von Karman Spectra of Vertical Gust Velocity from Severe Storm

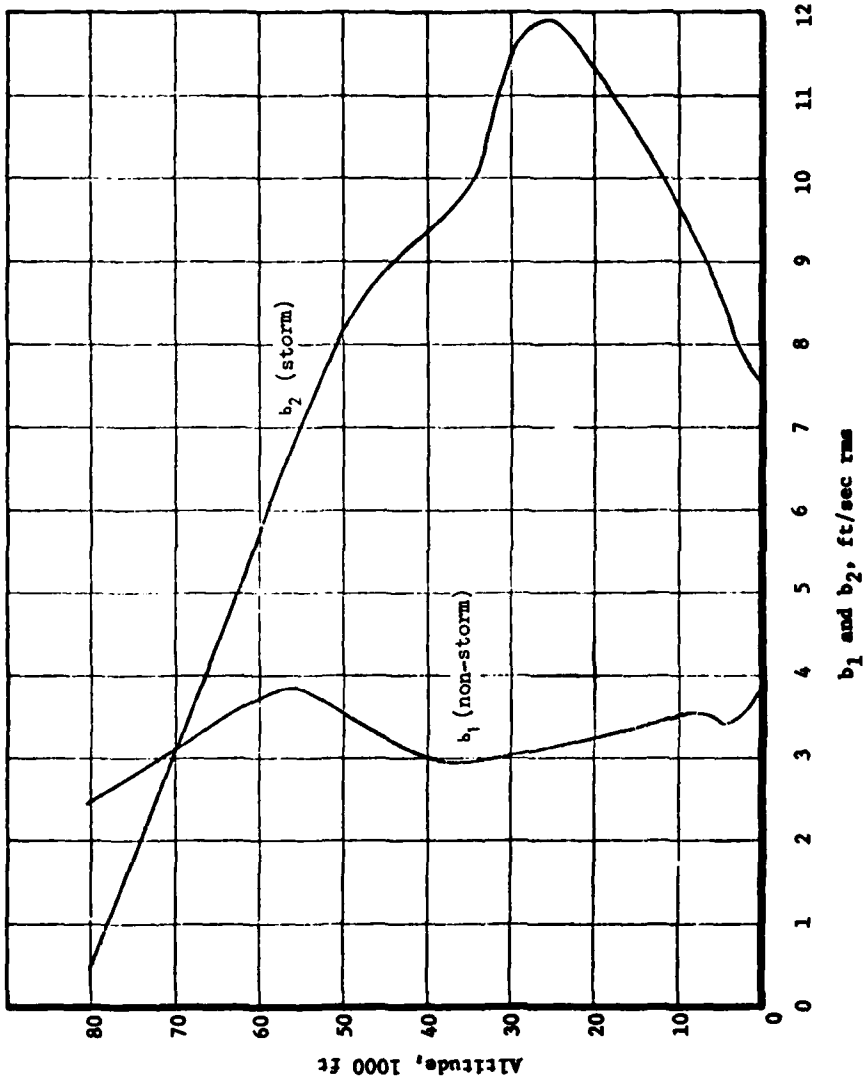

Figure 7. RMS Gust Velocity of Storm and Non-Storm Turbulence

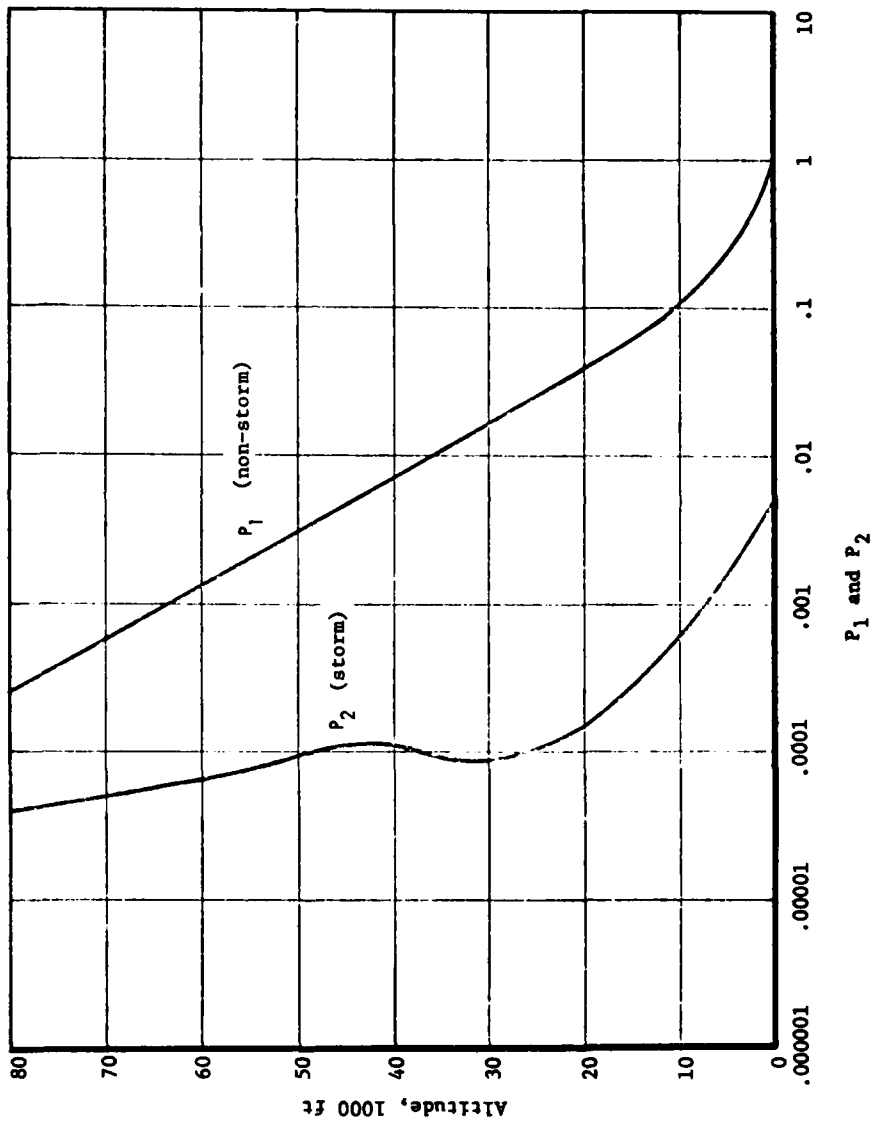

Figure 8. Probability of Storm and Non-Storm Turbulence

SECTION III
DYNAMIC ANALYSIS

When a stable system is driven by a steady sinusoidal input, the steady state response will be a sinusoid of the same frequency, and the phase angle of the response will differ from that of the excitation by some constant. If the complex amplitudes of the excitation and response are written in terms of the steady frequency of excitation, then the ratio of the response amplitude to the excitation amplitude is the "frequency response function."* The objective of the dynamic analysis is to formulate the frequency response function for a number of design parameters, such as loads, stresses, or accelerations at critical locations on the aircraft.

1. OVERVIEW

The starting point for a dynamic analysis is a complete description of a model of the aircraft in terms of geometry, stiffness, and mass properties. Normalized free-free airplane modes of vibration are calculated together with their associated frequencies. These normal modes together with rigid body modes are the basis for the generalized coordinate system of the analysis. All deflections which are possible for this model are representable as a sum of the products of the mode shapes, and suitable values of the corresponding generalized coordinates. The aerodynamic surfaces are modeled as a series of rigid panels, each of which is attached to the structural model. As the structure undergoes displacements, the panels move with respect to the free airstream and this gives rise to air forces on the various panels. The generalized

---

*The "frequency response function," "transfer function," and "mechanical admittance" are terms that are often used interchangeably. Strictly speaking, the frequency response function and the mechanical admittance refer to the same expression, but they are not necessarily the same as the transfer function. The transfer function will be the same expression only for the special case of a stable linear/invariant system subjected to steady sinusoidal excitation and viewed after all starting transients have vanished. However, this is the type of system under consideration.

mass and the inertia forces, due to displacements in the generalized coordinate system, are calculated. Because they are frequency dependent, generalized response and excitation air forces must be calculated for a distribution of frequencies over the frequency range in which significant aircraft response is possible.

The equations of motion are then formulated and solved for each frequency to give the frequency response in each of the generalized coordinates. The responses are the independent variables in a series of load equations that yield the design parameters which are the objective of the dynamic analysis.

2. LUMPED PARAMETER SYSTEM

The aircraft structure is a continuous distribution of mass and stiffness, and calculations of normal modes and frequencies on the basis of such a system is a formidable task. The equations of motion of a continuous system involve partial differential or integral equations which are relatively difficult to solve. Creation of a lumped parameter mathematical respresentation of the structure, or the use of finite elements, reduces the problem to one involving a finite number of simultaneous ordinary differential equations, which are easier to solve.

The basis for a lumped parameter or finite element representation of a continuous system is the assumption that deformations of the continuous structure may be approximated by deflections and rotations at a finite number of discrete points, and that the inertial properties of the structure may be represented by suitable masses and inertias located at these points. In the case of a wing of low aspect ratio, a two-dimensional array of points is often used in order to adequately represent the system. A high aspect ratio wing which is very stiff in the chordwise direction may often be adequately represented by points on a single line located along the elastic axis, with concentrated mass and inertia at each point.

3. MASS AND STIFFNESS MATRICES

The equations of motion for free vibration are most readily formulated in matrix form with mass and stiffness matrices. The mass matrix for a lumped parameter model is diagonal, with the lumped masses and inertias forming the diagonal. The masses are assumed to undergo deflections in only one direction - - normal to the plane of the surface, and inertias undergo rotations about only one axis. The stiffness matrix consists of both diagonal and off-diagonal terms and is somewhat difficult to calculate directly. The flexibility matrix, which is the inverse of the stiffness matrix, is relatively easy to formulate analytically, or to determine experimentally if the structure is available for test. The ith column of the flexibility matrix is the array of deflections (or rotations) at each of the mass points (or inertia locations), due to a unit load (or moment) applied to the ith mass point (or inertia location). Having formulated the flexibility matrix, the stiffness matrix may be obtained by matrix inversion. The finite element method allows the stiffness matrix to be formulated directly, and is often used for large structures.

4. NORMAL MODES

If structural damping, which has relatively small effects on aircraft mode shapes and frequencies is neglected, the differential equation for free vibration of an aircraft structure may be written as:

$$\left[M_f\right]\left\{\ddot{x}\right\} + \left[K_f\right]\left\{x\right\} = \left\{0\right\} \tag{16}$$

where

$\left[M_f\right]$ = Mass matrix

$\left[K_f\right]$ = Stiffness matrix

The assumption that the response of the system is simple harmonic motion reduces this differential equation to the following algebraic equation which has a non-trivial solution if, and only if, the determinant of the coefficient is zero:

$$\left[\left[K_f\right] - \omega^2\left[M_f\right]\right]\left\{x\right\} = \left\{0\right\} \tag{17}$$

The solution to this equation is a set of natural frequencies ω_{N_i}, and corresponding eigenvectors which satisfy the above equation.

When a large number of masses are used to represent the structure, the problem of calculating free-free normal modes directly becomes difficult. In this case, it is often advantageous to calculate modes and frequencies for each of the major components of the structure individually, and then to combine these so-called "cantilever modes" together with rigid body modes in a second eigenvalue problem to obtain the free-free aircraft modes. In deriving the cantilever modes, the point of attachment of the particular component to the main structure is assumed to be rigid. It is important that all of the cantilever modes whose frequencies are within the frequency range in which significant aircraft response is possible be determined in order to preserve accuracy in the final free-free modes.

5. EQUATIONS OF MOTION

The equations of motion written in terms of the generalized coordinates for the aircraft are a set of linear, nonhomogeneous, simultaneous differential equations of second order. The coefficient matrices consist of both aerodynamic and structural terms, and may be written as follows:

$$\left[M_S + M_A\right]\left\{\ddot{q}\right\} + \left[D_S + D_A\right]\left\{\dot{q}\right\} + \left[K_S + K_A\right]\left\{q\right\} = -\left\{C_0\right\} w_g(t) \quad (18)$$

where

$\left\{\ddot{q}\right\}, \left\{\dot{q}\right\}, \left\{q\right\}$ = acceleration, velocity, and displacement matrices of the generalized coordinates.

$w_g(t)$ = gust velocity

$\left\{C_0\right\}$ = modal force coefficient matrix per unit gust velocity

$\left[M_s\right]$ = generalized structural mass matrix

$\left[M_a\right]$ = generalized aerodynamic mass matrix

$\left[D_s\right]$ = generalized structural damping matrix

$\left[D_a\right]$ = generalized aerodynamic damping matrix

$\left[K_s\right]$ = generalized structural stiffness matrix

$\left[K_a\right]$ = generalized aerodynamic stiffness matrix

The structural coefficient matrices are all diagonal matrices as a result of selecting normal modes as a basis for the generalized coordinate system. The generalized mass may be calculated from the following summation over N masses representing the entire aircraft:

$$M_{S_{ii}} = \sum_{j=1}^{N} \phi_{ij}^2 m_j \tag{19}$$

where

ϕ_{ij} = the deflection at the jth lumped mass due to a unit deflection in the ith generalized coordinate

m_j = *mass of the jth lumped mass*

For the rigid body translation modes, $\phi_{ij} = 1$, and the resulting term in the generalized mass is equal to the mass of the aircraft The coordinate system for rigid body rotation modes must be the principal axis of the aircraft in order to preserve orthogonality. For these modes, the generalized mass term is the normalized mass moment of inertia about the appropriate principal axis.

The structural contribution to the generalized stiffness is calculated from the generalized mass as follows:

$$K_{S_{ii}} = M_{S_{ii}} \omega_{N_i}^2 \tag{20}$$

where

ω_{N_i} = natural frequency of the ith normal mode.

The natural frequency for the rigid body modes is zero, hence the generalized stiffness matrix is singular.

Structural damping results from friction within the structure, particularly at joints between components. Unlike viscous damping forces, these damping forces are proportional to the strain of the system, yet are in phase with the velocity. This contribution may be formulated as follows:

$$\left[D_S\right]\left\{\dot{q}\right\} = i\left[g\right]\left[K_S\right]\left\{q\right\}. \tag{21}$$

As a result of assuming simple harmonic motion:

$$\left\{\dot{q}\right\} = i\omega\left\{q\right\} \tag{22}$$

Substitution gives:

$$\left[D_S\right]\left\{\dot{q}\right\} = \frac{1}{\omega}\left[g\right]\left[K_S\right] \tag{23}$$

Hence:

$$\left[D_S\right] = \frac{1}{\omega}\left[g\right]\left[K_S\right] \tag{24}$$

The damping coefficient matrix $\left[g\right]$ is determined from vibration tests, when available; or is assumed to be about 5% of critical damping.

6. LOAD EQUATIONS

Load equations for calculating the design parameters which are the objective of the dynamic analysis are similar in form to the equations of motion, and may be expressed as:

$$\left\{R\right\} = \left[M_R\right]\left\{\ddot{q}\right\} + \left[D_R\right]\left\{\dot{q}\right\} + \left[K_R\right]\left\{q\right\} + \left\{C_R\right\} w_g(t) \tag{25}$$

where

$\left[M_r\right]$ = generalized mass matrix for response load equations

$\left[D_r\right]$ = generalized damping matrix for response load equations

$\left[K_r\right]$ = generalized stiffness matrix for response load equations

$\left\{C_r\right\}$ = modal force coefficient matrix for response load equations

These equations are formulated by transforming the generalized inertia, damping, and stiffness forces into loads, stresses, accelerations, etc., per unit deflection of the generalized coordinates.

7. AERODYNAMIC FORCES

The generalized external forces which result from the motion of the system may be expressed as a column matrix of modal forces $\left\{Q_R\right\}$ These forces may be calculated from the following matrix equation:

$$\left\{Q_R\right\} = \left[\phi^T\right]\left[G\right]\left[A\right]\left[\phi\right]\left\{q\right\} \tag{26}$$

where

$\left[\phi\right]$ = transformation from displacements of the generalized coordinate system to displacements at the aerodynamic panels, generally referred to as mode shapes.

$\left[G\right]$ = complex transformation from two-dimensional panel forces to three-dimensional panel forces which includes finite time delays for the transmittal of induced lifts, generally referred to as dynamic induction matrix.

$\left[A\right]$ = oscillatory panel forces per unit sinusoidal panel displacements, generally referred to as lift and moment matrix.

Selecting an excitation frequency, ω, and evaluating the foregoing generalized external force results in a matrix with complex coefficients. The assumption of simple harmonic motion allows this expression to be successively expanded as:

$$\left\{Q_R\right\} = \left[a + ib\right]\left\{q\right\} = \left[a\right]\left\{q\right\} + \frac{1}{\omega}\left[b\right]\left\{\dot{q}\right\} \tag{27}$$

The aerodynamic stiffness matrix, $\left[K_a\right]$, results from those air forces which are in phase with the generalized coordinates, and the aerodynamic damping matrix, $\left[D_a\right]$, results from those air forces which are 90-degrees out of phase with the generalized coordinates. Hence:

$$\left[K_A\right] = \text{REAL PART OF} \left[\phi^T\right]\left[G\right]\left[A\right]\left[\phi\right] \tag{28}$$

and:

$$\left[D_A\right] = \text{IMAGINARY PART OF } \frac{1}{\omega}\left[\phi^T\right]\left[G\right]\left[A\right]\left[\phi\right] \tag{29}$$

Although the mass of the air in close proximity to the aerodynamic surface does impart inertial forces to the surface itself, this contribution is negligible compared with the mass of the structure. Therefore, $\left[M_a\right]$ is assumed to be zero:

$$\left[M_A\right] = \left[0\right] \tag{30}$$

The remaining external forces arise from the gust induced angle of attack $\alpha_g(t)$. A phase angle delay, which is proportional to the panel location aft of some reference point, appears in the expression in order that the effects of the gust will be felt progressively along the flight path at a speed equal to the velocity of the aircraft. Hence, for a sinusoidal gust field of frequency ω and maximum amplitude w_g, the gust induced angle of attack for the various panels may be expressed as:

$$\left\{\alpha_g(t)\right\} = \frac{w_g}{V_T} e^{i\omega t}\left\{e^{i\theta}\right\} = \frac{w_g(t)}{V_T}\left\{e^{i\theta}\right\} \tag{31}$$

where

V_T = true velocity of the aircraft

$\theta = \frac{\omega\lambda}{V_T}$ = phase angle delay for each panel

λ = panel location aft of some aircraft reference point

The form of the final equation for gust induced external forces, $\{Q_g\}$, is similar in form to the expression for the response external forces, the essential difference being the $[\phi]$ $\{q\}$ is replaced by $\{\alpha_g(t)\}$. Hence:

$$\{Q_g\} = [\phi^T][G][A_g]\{\alpha_g(t)\} \tag{32}$$

where

$[A_g]$ = oscillatory panel forces per unit sinusoidal angle of attack

From this equation, the complex column matrix $\{C\}$ in the equations of motion is given by:

$$\{c\} = \frac{1}{V_T}[\phi^T][G][A_g]\{e^{i\theta}\} \tag{33}$$

8. AERODYNAMIC THEORIES

A number of aerodynamic theories of various degrees of complexity are available to calculate the oscillatory panel forces. The "doublet-lattice" (Reference 5) is an example of one of the more complex theories, and calculations based on this theory agree well with tests. The aerodynamic surfaces are divided into a series of trapezoidal "panels" by a series of lines parallel to the free stream, and a series of lines of roughly constant percent chord. On each panel, a steady "horseshoe vortex" is used to develop the steady portion of the lift, and a line of oscillatory "doublets" is used to represent the oscillatory portion. The horseshoe vortex is located so that the bound segment of the vortex coincides with the quarter-chord of the panel and the parallel segments of the vortex trails from the ends of the quarter-chord of the panel in the free stream direction. The lines of oscillatory doublets coincide with the quarter-chord of the panel. "Downwash collocation" points are located on the three-quarter-chord of each panel, centered spanwise. The downwash from each of the vortices and doublets is summed at each collocation point and the component normal to the surface is

equated to zero. This results in a system of simultaneous equations, the solution of which gives the aerodynamic forces on each of the panels, per unit oscillatory deflection at a given frequency.

9. SOLUTION TO THE EQUATIONS OF MOTION

A solution for the equations of motion is required for a distribution of frequencies from near zero to the highest frequency at which significant structural response is possible. Combining the structural and aerodynamic terms into single unsubscripted terms yields the following equation:

$$[M]\{\ddot{q}\} + [D]\{\dot{q}\} + [K]\{q\} = -\{c_o\} w_g(t) \qquad (34)$$

The response of a linear system to steady sinusoidal excitation will be simple harmonic motion at the same frequency as the excitation, but with some finite phase angle between the excitation and response. Hence:

$$\{q\} = \{q_o\} e^{i\omega t + \phi} \qquad (35)$$

when

$$w_g(t) = e^{i\omega t} \qquad (36)$$

where $\{q_o\}$ is the maximum amplitude of the steady sinusoidal response, and ϕ is the phase angle between the excitation and response. Successive differentiation of the modal displacement gives the modal velocity and acceleration as:

$$\{\dot{q}\} = i\omega\{q_o\} e^{i\omega t + \phi} \qquad (37)$$

and

$$\{\ddot{q}\} = -\omega^2\{q_o\} e^{i\omega t + \phi} \qquad (38)$$

Substituting the modal displacement, velocity, and acceleration into the equation of motion and dividing by $e^{i\omega t + \phi}$ yields:

$$\left[\left[K\right] - \omega^2\left[M\right] + i\omega\left[D\right]\right]\left\{q_o\right\} = -\left\{c_o\right\} \tag{39}$$

From which the solution is:

$$\left\{q_o\right\} = -\left[\left[K\right] - \omega^2\left[M\right] + i\omega\left[D\right]\right]^{-1}\left\{c_o\right\} \tag{40}$$

The right-hand side of the foregoing equation is the frequency response function of that part of the system which relates the modal displacement to the sinusoidal gust velocity:

$$\left\{H(i\omega)\right\} = \left[\left[K\right] + (i\omega)^2\left[M\right] - (i\omega)\left[D\right]\right]^{-1}\left\{c_o\right\} \tag{41}$$

Frequency Response Function

If it were not for the aerodynamic contribution to the damping and stiffness matrices, the frequency response function for this system would display a single peak as does the frequency response function for a single degree-of-freedom damped oscillator, which when normalized appears as in Figure 9 (Reference 6).

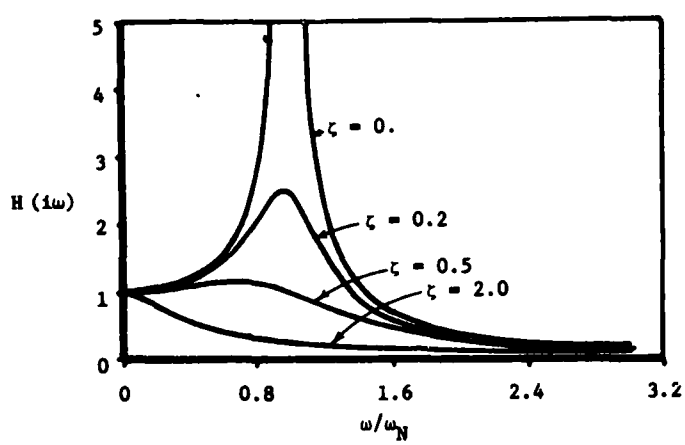

Figure 9. Frequency Response Function of Simple Damped Oscillator

where

$H(i\omega)$ = frequency response function for single degree-of-freedom damped oscillator

ζ = ratio of actual damping to critical damping

ω_n = undamped natural frequency

ω = sinusoidal excitation frequency

The significance of the off-diagonal contribution of the aerodynamic terms to the damping and stiffness matrices is to create cross-coupling between the normal modes. Figure 10 (Reference 7) shows the frequency response function of the modal displacement of the first symmetrical flexible free-free mode of vibration of a commercial transport aircraft.

10. SOLUTION TO THE LOAD EQUATIONS

A solution to the load equations is obtained from the solution to the equations of motion, using the same assumptions of simple harmonic motion. Substituting the modal displacement, velocity, and acceleration written in terms of $\{q_o\}$ into the load equations, collecting terms, and dividing by $e^{i\omega t + \phi}$ yields:

$$\{R_o\} = \left[\left[K_R\right] - \omega^2\left[M_R\right] + i\omega\left[D_R\right]\right]\{q_o\} + \{C_R\} \qquad (42)$$

where

$\{R_o\}$ is the maximum amplitude of the steady sinusoidal response

and

$\{q_o\}$ is the solution to the equations of motion.

The frequency response functions for the design parameters display the same multi-peak characteristics as the frequency response function of the normal coordinates. Figure 11 shows the frequency response function for wing bending moment at 1/3 span of a commercial transport aircraft subject to vertical gust excitation of one foot per second rms.

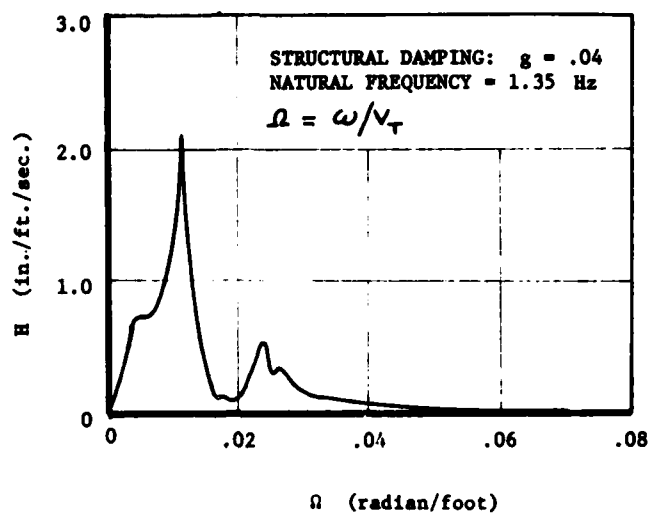

Figure 10. Frequency Response Function of First Free-free Airplane Mode of Vibration

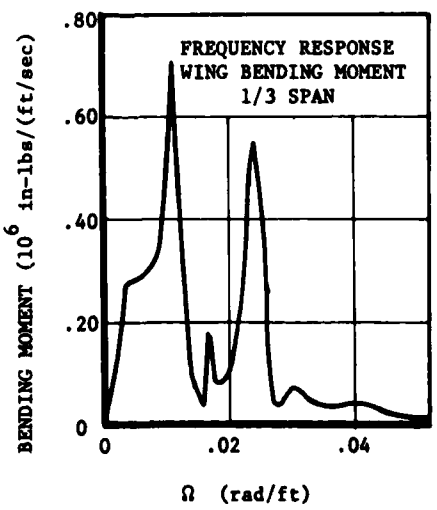

Figure 11. Frequency Response of Wing Bending Moment at 1/3 Span

SECTION IV
SPECTRAL ANALYSIS

For a linear system excited by a random function which is both Gaussian and stationary, the PSD of the output is expressed in terms of the PSD of the input by the following equation:

$$\phi_{output} = |H|^2 \phi_{input} \tag{43}$$

where

H = frequency response function

The relative simplicity of this equation has motivated the assumptions that atmospheric turbulence may be characterized as a stationary random process whose gust amplitudes have a Gaussian distribution, and that the flight of an aircraft through the atmosphere may be characterized as a linear system represented by a frequency response function.

The concept of stationarity that is implied is that the statistical properties of the input averaged over a short time interval do not vary significantly from one interval to another. This concept is sometimes called "self-stationarity" to avoid confusion with the more classical definition of stationarity which involves averages over an "ensemble" (Reference 8) of functions, rather than averages in time along a single function.

If X(t) characterizes a velocity component of atmopsheric turbulence, then the Gaussian assumption implies that the probability distribution of X(t) may be expressed in terms of two parameters -- the "variance" and the "mean value." This distribution has a bell shape given by the following expression:

$$p(x) = \left(\sigma_x \sqrt{2\pi}\right)^{-1} \text{EXP}\left[\frac{\left(x(t) - \mu_x\right)^2}{2\sigma_x^2}\right] \tag{44}$$

where

$$\mu_x = \frac{1}{T}\int_0^T X(t)\,dt = \text{mean value of } X(t)$$

$$\sigma_x = \frac{1}{T}\int_0^T \left(X(t) - \mu_x\right)^2 dt = \text{variance of } X(t)$$

$p(x)$ = probability density of $X(t)$

Accepting these assumptions, the power spectral relation for the response of an aircraft becomes:

$$\phi_R(\omega) = \left|H(i\omega)\right|^2 \phi(\omega) \tag{45}$$

where

$\phi(\omega)$ = PSD of the atmosphere as detailed in Section II

$H(i\omega)$ = frequency response function of the design parameters as detailed in Section III

$\phi_R(\omega)$ = PSD of the design parameter

Two real and positive parameters are calculated from the power spectrum of each of the design parameters for use in the design process. The first parameter, $\bar{A}$, is the rms response per unit rms turbulence intensity, and it is the square root of the area under the response parameter power spectrum. The second parameter, N_0, is a characteristic frequency, calculated from the first moment of the area under the PSD curve about the zero frequency line. It is the expected number of exceedances of the zero load level per unit time. These expressions are:

$$\bar{A} = \sqrt{\int_0^\infty \phi_R(\omega)\,d\omega} \tag{46}$$

and:

$$N_0 = \frac{\sqrt{\int_0^\infty \omega^2 \phi_R(\omega)\,d\omega}}{2\pi\,\bar{A}} \tag{47}$$

1. DESIGN ENVELOPE ANALYSIS

In the PSD design envelope analysis, it is assumed that the ratio of the "correct" design value to the rms design value is a constant η_d. If the design value for rms turbulence intensity is σ_w, then the rms response is $\sigma_w\bar{A}$, so that the "correct" design value is (Reference 9):

$$y_d = \sigma_w \eta_d \bar{A} \tag{48}$$

In practice, σ_w and η_d need not be considered separately and their product is defined as U_σ, the nominal turbulence intensity. The design value for the design parameters becomes:

$$y_d = U_\sigma \bar{A} \tag{49}$$

Acceptable values of U_σ may be determined from the analysis of previous aircraft which were gust critical, and have demonstrated a long service life. $\bar{A}$ is calculated and the foregoing equation is solved for U_σ when y_{design} is set equal to the limit allowable value of the design parameter:

$$U_\sigma = \frac{y_{LA} - y_{1-g}}{\bar{A}} \tag{50}$$

where

y_{LA} = limit allowable value for design parameter

y_{1-g} = value of the design parameter in steady level (1-g) flight

$\bar{A}$ = rms response of design parameter per unit rms gust excitation

In an effort to establish acceptable values of U_σ, the Federal Aviation Administration sponsored a study of a number of proven aircraft designs. Company engineering staffs determined the value of U_σ that would produce the limit allowable stress value at the most critical location on each aircraft. This amounts to selecting the lowest value of U_σ from the analysis of all of the locations which were considered to be

potentially critical. The results of two such analyses are listed below (Reference 4):

AIRCRAFT MODEL	U_σ VERTICAL GUST	ALTITUDE
Boeing 707-720B	111 ft/sec	22000 ft
Lockheed 749	88 ft/sec	7000 ft

Based on this type of analysis, the following values of U_σ as a function of altitude has been established. The solid lines are proposed standards applicable to commercial transport category aircraft, and the dotted line is the requirement of the US Air Force (Reference 10).

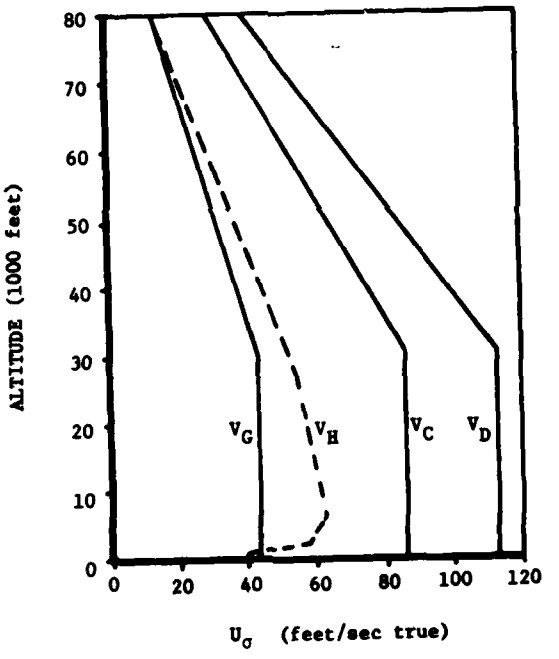

Figure 12. Derived Gust Velocity for Design Envelope Analysis

where

V_G = gust penetration velocity (civil aircraft)

V_H = maximum continuous velocity in steady level flight (military aircraft)

V_C = maximum cruise velocity (civil aircraft)

V_D = maximum dive velocity (civil aircraft)

2. MISSION ANALYSIS

The mission analysis permits the intended usage of the aircraft to be reflected in the design. The objective of the mission analysis is to establish design levels so that during the intended operation of the aircraft, the expected number of exceedances of specific load levels per hour of operation do not exceed an acceptable value.

The basis for the mission analysis is the assumption that both storm and non-storm turbulence occur in patches, where each patch is a stationary, Gaussian random process with a particular rms turbulence intensity σ. Although σ is a constant within each patch, it is assumed that the distribution of σ's from the various patches in both categories of turbulence is Gaussian. For a single patch, the number of exceedances per unit time of level y is given by Equation 51. This equation is derived in Appendix A using Houbolt's approach (Reference 11).

$$N(y) = N_0 \, e^{\frac{-y^2}{2\sigma_y^2}} \tag{51}$$

where

N_0 = expected number of exceedances of the level y = 0 per unit of time

σ_y = rms response of design parameter

y = level of response design parameter for which exceedances are calculated

Invoking the assumption that the various values of σ from each category have a Guassian distribution results in the following modification of the foregoing equation:

$$N(y) = N_0 \left\{ P_1 \, e^{\frac{-y}{\bar{A} b_1}} + P_2 \, e^{\frac{-y}{\bar{A} b_2}} \right\} \tag{52}$$

where

P_1, P_2 = probability of encountering turbulence of non-storm and storm category respectively

b_1, b_2 = rms turbulence intensity of non-storm and storm turbulence respectively

$\bar{A}$ = rms response of the design parameter per unit rms turbulence excitation

A detailed derivation of the foregoing equation is presented in Appendix A. In the mission analysis design process, it is assumed that the operation of the aircraft consists of a specified number of flights where each flight is one of a limited number of "missions." The ratio of the number of flights of the various missions to the total number of flights is called the "mission mix," which is specified as part of the design requirements. Examples of some missions that might be included in the design of fighter aircraft include:

1. Ferry
2. Training
3. Combat
4. Reconnaissance

Each mission is created by linking together a number of "mission segments" which is often illustrated in a plot of altitude vs time such as the plot on the following page. Typical mission segments which might be included in one or more missions are:

1. Takeoff
2. Climb
3. Cruise
4. Loiter
5. Air to air combat maneuvers
6. Air to ground combat maneuvers
7. Descent
8. Landing

Having decided upon how many flights of each mission will be flown during the life of the aircraft, and how each mission is assembled in terms of mission segments, a composite mission is established which has the same ratio of the various mission segments as the sum of all of the flights planned for the lifetime of the aircraft. If T is the duration of the composite mission and T_i is the duration of the ith mission segment in the composite mission, then define t_i to be that fraction of time for the ith mission segment in the composite mission:

$$t_i = \frac{T_i}{T} \tag{53}$$

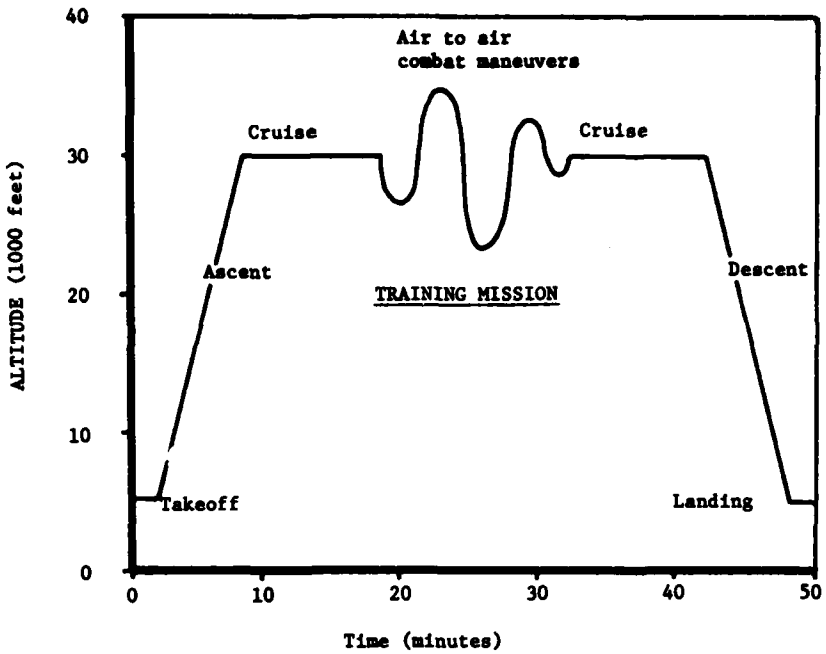

Figure 13. Mission Profile of Training Mission

The average number of exceedances per unit time for the composite mission will be given by:

$$N(y) = \sum_{\substack{\text{mission} \\ \text{segments}}} N_{o_i} t_i \left[P_1 e^{\frac{-y}{b_1 \bar{A}_i}} + P_2 e^{\frac{-y}{b_2 \bar{A}_i}} \right] \tag{54}$$

A plot of N(y) vs y results in an exceedance curve of the following form:

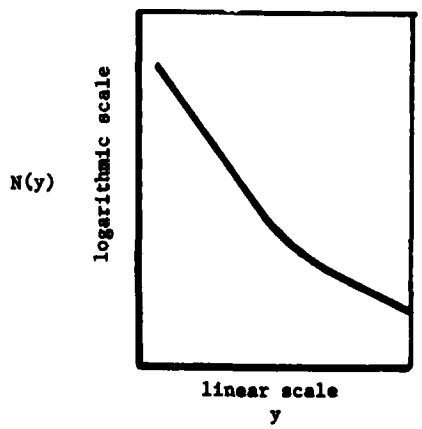

Figure 14. Typical Exceedance Curve

There is no practical load level for which the number of exceedances will be zero, hence, in order to utilize the above result, an acceptable number of exceedances of some particular load level must be established.

Company engineering staffs have calculated the expected number of exceedances of limit strength per hour of operation of a number of successful aircraft, and the results of two such analyses are as follows (Reference 4):

AIRPLANE MODEL	EXCEEDANCES OF LIMIT LOAD PER HOUR Vertical Gust	Lateral Gust
Boeing 707-720B	1.1×10^{-5}	4.0×10^{-6}
Lockheed 749	1.8×10^{-5}	2.5×10^{-4}

The appropriate design level for the number of exceedances of limit load per hour of operation due to vertical gust was selected to be (Reference 10):

$$N(y) = 2.0 \times 10^{-5} \tag{55}$$

which amounts to one exceedance of limit load per 50,000 hours of operation. This is currently the requirement for US Air Force aircraft and is the proposed standard for civil transport aircraft.

SECTION V
NONSTATIONARY TURBULENCE MODELS

The stationary assumption has been made in order to simplify aircraft response calculations, but this assumption is not entirely satisfactory. The initial encounter with a gust field is often characterized by rapid changes in the statistical properties of the aircraft response parameters with time, and these properties may vary continuously while the aircraft is in turbulence. This effect cannot be accounted for in a stationary analysis. Indeed, the analysis of real data indicates that the traditional PSD procedure consistently underestimates the number of exceedances of the higher load levels due to turbulence.

The degree to which the traditional analysis underestimates the number of exceedances in these higher load levels has, on occasion, been exaggerated. Some of the reports on the inadequacy of the traditional analysis are the result of a lack of understanding, and it is appropriate to expose some of these misconceptions.

The most flagrant misconception is that the present analysis is entirely Gaussian. The number of exceedances versus load levels for a single, stationary, Gaussian process is compared to points indicative of real data in Figure 15.

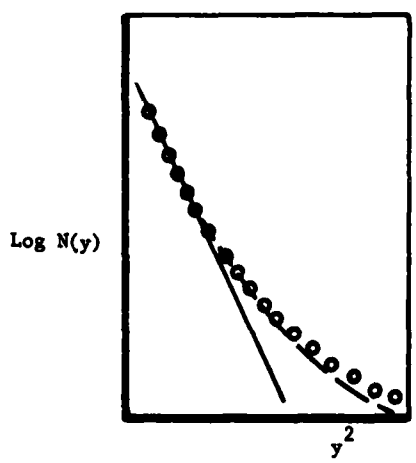

Figure 15. Gaussian Exceedance Curve

The single stationary, Gaussian process plots as a straight line in Figure 15, whereas a distribution of Gaussian, stationary patches plots as shown by the dashed line, resulting in a considerably better fit to the points indicative of real data.

On other occasions, the fact that the Gaussian Patch model assumes that the mean square intensity of the various patches come from two different processes (storm and non-storm), has not been recognized. The significance of this assumption appears in Figure 16.

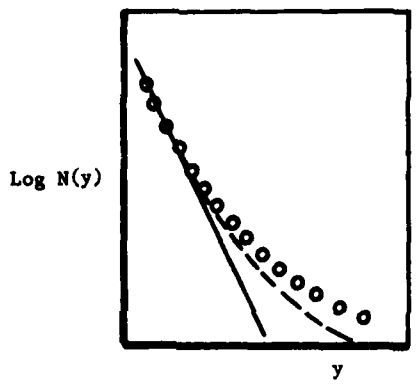

Figure 16. Gaussian-Patch Exceedance Curve

In this figure, the Gaussian-patch model from a single distribution is the solid straight line. However, when two distributions are considered, it plots as the dashed line. Although the use of two distributions give results which are considerably better, the number of exceedances of the higher load levels is still underestimated. However, the difference is usually considered to be negligible.

Other analyses of data have permitted three distributions to be used, where the third distribution accounts for the very rare occurrence of extreme turbulence (Reference 12). In view of the added complexity of including a third distribution, the value of such a distribution can be debated.

1. TRANSIENT OVERLOADS

In the Gaussian-patch analysis, the transients resulting from the transition from one patch to another are not considered. The stationarity assumption has been questioned on the basis that it may ignore significant transient overloads. At least one study has indicated that transient response in excess of 30% above the stationary response has been observed (Reference 13). The analysis utilized a nonstationary model for turbulence of the following form:

$$w(t) = a(t)\ z(t) \tag{56}$$

where

$a(t)$ = a deterministic modulating function

$z(t)$ = spectrally shaped, Gaussian white noise

$w(t)$ = nonstationary, possibly non-Guassian turbulence

The modulating function $a(t)$ that was used was a ramp function of the following form:

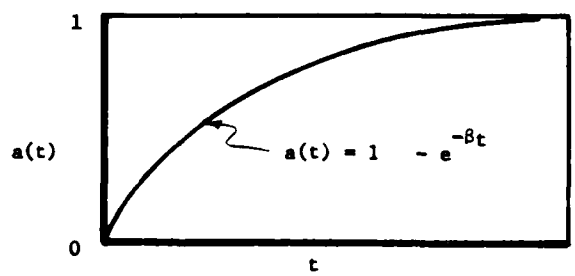

Figure 17. Modulating Function

The high transient was observed utilizing an enveloping function with an extremely short rise time (90% in .01 seconds) as compared with the natural response time of the aircraft model. In effect, the aircraft was probably subjected to a severe discontinuity as indicated in Figure 18.

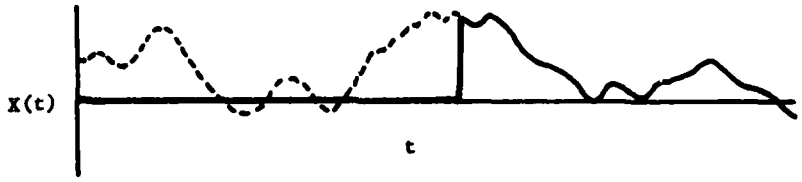

Figure 18. Nonstationary Excitation Function

The dashed line represents the function z(t) and the solid line represents the product of z(t) and a(t).

In summary, the Gaussian-patch model fails to predict the number of exceedances of the higher load levels, but the magnitude of this deficiency is small for many applications to gust design problems.

2. UNIFORMLY MODULATED PROCESS

Past efforts to model atmospheric turbulence as a nonstationary process have included the notion that turbulence may be represented as a stationary Gaussian random process modulated by an enveloping function as follows:

$$w(t) = f(t)\ z(t) \tag{57}$$

where

f(t) = discrete modulating function

z(t) = Gaussian white noise that has been spectrally shaped

w(t) = nonstationary, possibly non-Gaussian turbulence

A variety of enveloping functions can be devised which are thought to represent a number of different types of nonstationary turbulence encounters. This model is referred to as "uniformly modulated" and is particulary attractive because a Fourier series may be used to express the enveloping function, and equations for the statistical properties of the response parameters (including the number of exceedances per unit time) may be derived in closed form.

Another approach, which could be considered to be an expansion of the uniformly modulated process, is to model turbulence in the following form (Reference 14):

$$w(t) = f(t)\, z(t) + g(t) \tag{58}$$

where z, f, and g are independent stationary Gaussian processes. In effect, g(t) is the time varying mean value of the turbulence and f(t), although random, performs a similar function to that of f(t) in the uniformly modulated process; z(t) is the same for both models. This more complicated model has an advantage in that it gives a less uniform structure, and thus has an "appearance" more like that of real turbulence.

3. TIME VARYING POWER SPECTRA

Other approaches which are computationally more difficult, embody the concept of a time-varying power spectrum. The "evolutionary power spectrum" first presented by M. B. Priestly is of the form (Reference 15):

$$\phi(t,\Omega) = \left|A(t,\Omega)\right|^2 \phi(\Omega) \tag{59}$$

where

$\phi(\Omega)$ = stationary power spectrum of the atmosphere, i.e., the von Karman or Dryden spectrum

$A(t,\Omega)$ = time varying transfer function

$\phi(t,\Omega)$ = evolutionary power spectrum

The time-varying transfer function performs a similar operation in the frequency domain to what the enveloping function of the uniformly modulated function performed in the time domain.

W. D. Mark has made use of the fact that the autocorrelation function and the PSD function are Fourier transform pairs (Reference 16). For the stationary case;

$$R(\tau) = \int_{-\infty}^{\infty} e^{i\omega\tau} \phi(\omega)\, d\omega \tag{60}$$

and:

$$\phi(\omega) = \frac{1}{2\pi} \int_0^\infty e^{-i\omega\tau} \, d\tau \tag{61}$$

Mark obtained a time varying autocorrelation function and then utilized the Fast Fourier Transform (FFT) technique to obtain the time varying "instantaneous power spectrum."

Recently, Mark and Fisher investigated the effects of nonstationary behavior on the spectra of atmopsheric turbulence using the instantaneous power spectrum (Reference 16). They concluded that the shape of the von Karman spectrum will be virtually unchanged when the enveloping function of the uniformly modulated process is sufficiently well behaved that:

$$L^2 \left| \frac{d^2}{dt^2} \left(\mathrm{Ln}\, \sigma(t) \right) \right| \leq 0.04 \tag{62}$$

where

L = scale of turbulence of the von Karman spectrum

$\sigma(t)$ = time-varying mean value (enveloping function)

Mark and Fisher arrived at this conclusion by starting with an expression for the instantaneous power spectra of a uniformly modulated process:

$$\phi(\Omega, t) = \left[\sigma(t) \right]^2 \phi(\Omega) \tag{63}$$

They derived a new series expansion for the instantaneous spectra and wrote the first two terms as:

$$\phi(\Omega, t) \approx \sigma^2(t) \left[\phi(\Omega) - \frac{1}{16\pi^2} \frac{d^2}{dt^2} \left(\mathrm{Ln}\, \sigma(t) \right) \phi^2(\Omega) \right] \tag{64}$$

Note, that this results in the regular power spectra when $\sigma(t)$ is constant, and thus the second term displays the results of any nonstationary fluctuations in the modulating function $\sigma(t)$.

In order to determine the magnitude of the second term necessary to produce a noticeable change in the power spectrum, Mark and Fisher generated a number of nonstationary samples (i.e., time series) from a uniformly modulated process, and compared the power spectra of these samples to the power spectra of "Gaussian equivalent" samples. In this investigation Gaussian equivalent samples were constructed such that the crossings of the zero load level in time were identical to that of the nonstationary samples, yet the distribution of amplitudes was Gaussian. Mark and Fisher utilized the so-called "arc-sine law" to construct the Gaussian-equivalent samples. This law states that:

$$R_z(\tau) = \mathrm{SIN}\left[\frac{\pi}{2} R_{o_z}(\tau)\right] \tag{65}$$

where

$R_z(\tau)$ = autocorrelation function of a Gaussian (possibly non-stationary) random process $z(t)$

$R_{o_z}(\tau)$ = autocorrelation function of a process whose magnitude is +1 when $z(t) > 0$, and -1 when $z(t) < 0$. Therefore, the zero crossings will be identical to $z(t)$.

Figure 19 illustrates the procedure used. The magnitude of the first term was compared to the value of the second term in making the evaluation.

4. SELF-SIMILARITY

Self-similarity is a concept which may some day produce a model which characterizes both the nonstationary and non-Gaussian aspects of atmospheric turbulence. Whereas, the concept of stationary implies that the turbulence is invariant with respect to addition of time, the concept of self-similarity implies that turbulence is invariant with respect to multiplication of time (Reference 17). Specifically, a process with random variable x is self-similar if there exists some function F(h) such that the probabilistic structure of x is unchanged when the wavelength is multiplied by h and the amplitude by F(h).

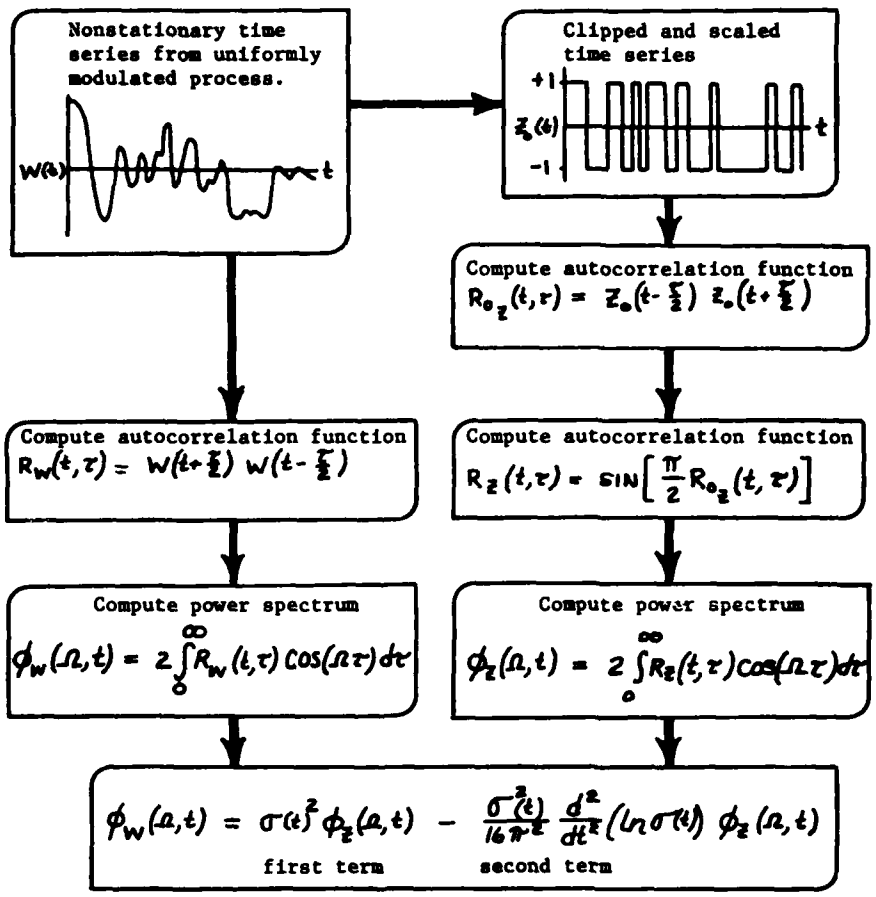

Figure 19. Procedure to Determine Effects of Nonstationary Excitation on the Spectra of Atmospheric Turbulence

That part of the power spectrum of atmospheric turbulence which displays a constant -5/3 slope on a log-log plot is referred to as the "inertial subrange." As shown in Appendix B, this characteristic -5/3 slope dictates that the self-similar function for the inertial subrange must be:

$$F(h) = h^{1/3} \tag{66}$$

This implies that if the temporal scale of a turbulence sample is expanded by a factor of 2 and the amplitude is increased by a factor of $2^{1/3}$, the resulting turbulence sample will have the same probabilistic structure. Dutton and Deavon (Reference 17) tested for self-similarity in turbulence samples by comparing segments of the same sample separated by various distances. Agreement was very good for separations of up to 50 meters. The failure of the self-similar concept at greater separations can possibly be attributed to a high spectral content of low-frequency waves that are outside of the inertial subrange. It may be possible to filter turbulence samples and then apply the appropriate similarity functions for the various frequency bands.

SECTION VI
CONCLUSIONS

The traditional PSD analysis for calculating the response of an aircraft to continuous turbulence was reviewed with special attention to the underlying assumptions. The degree to which the analysis reputedly underestimates the number of occurrences of turbulence in the higher load levels was challenged. It was shown that certain misconceptions are responsible for gross errors, although it was conceded that even a properly applied analysis may under-predict the number of occurrences of extreme turbulence. The error is reported to be negligible for many applications. Efforts to refine the procedure by modeling atmospheric turbulence as a nonstationary process are reviewed.

APPENDIX A
DERIVATION OF EXCEEDANCE EQUATION

This appendix presents a derivation of the following equation, which is an expression for the expected number of exceedances of a given load level per unit time:

$$N(y) = N_o \left\{ P_1 e^{\frac{-y}{\bar{A} b_1}} + P_2 e^{\frac{-y}{\bar{A} b_2}} \right\} \tag{67}$$

where

N_o = expected number of exceedances of the zero load level per unit time

P_i = probability of encountering turbulence of type i

b_i = rms intensity of turbulence of type i

$\bar{A}$ = rms response of design parameter per unit rms turbulence intensity

y = load level of design parameter for which exceedances are calculated

The first part of this derivation is attributed to John C. Houbolt (Reference 11). Turbulence is assumed to occur in patches where each patch is a stationary Gaussian process. Consider a portion of the response time history of one of the design parameters:

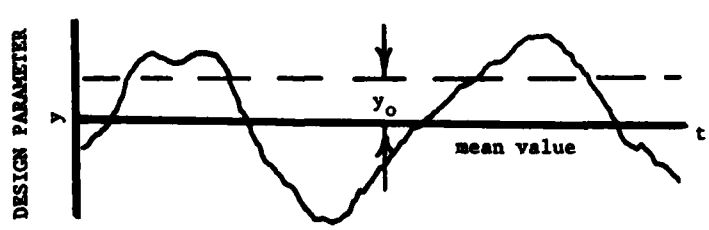

Figure 20. Typical Response Time History

Examine a typical crossing of the load level y_o in order to determine how much time is spent in a narrow band between y_o and $y_o + \Delta y$.

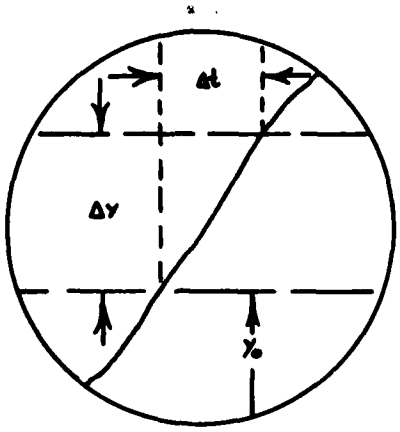

Figure 21. Typical Level Crossing

If the velocity of the crossing is $\dot{y}$, then the time required for an upward or downward crossing is:

$$(\Delta t)_o = \frac{\Delta y}{|\dot{y}_o|} \tag{68}$$

In an arbitrary length of time T_i, the amount of time spent in the incremental area of hyper-space (Δy) $(\Delta \dot{y})$ is by definition:

$$\Delta T = T_i \; p(y, \dot{y}) \; \Delta y \; \Delta \dot{y} \tag{69}$$

where

$p(y,\dot{y})$ = joint probability distribution between y and $\dot{y}$

$$y = y_o = \text{fixed value}$$

The number of crossings of the interval Δy in time T_i will then be:

$$dn = \frac{\Delta T}{(\Delta t)_o} = T_i \, |\dot{y}| \; p(y, \dot{y}) \, d\dot{y} \tag{70}$$

The number of exceedances of the level y will be equal to the number of crossings in one direction -- either with positive or negative velocity, but not both. For convenience, consider only upward crossings and therefore integrate over positive values of velocity.

$$n = T_i \int_0^\infty \dot{y}\ p(y,\dot{y})\,d\dot{y} \tag{71}$$

An aircraft spends only part of the time in turbulence of a particular type; let P_i be the ratio of that amount of time to the total amount of flight time:

$$P_i = \frac{T_i}{T} \tag{72}$$

where

T_i = amount of time in turbulence of type i

T = total amount of flight time

P_i = portion of flight time in turbulence of type i

Hence, the total number of exceedances of level y per unit time is given by:

$$N = \sum_i P_i \int_0^\infty \dot{y}_i\ p(y_i,\dot{y}_i)\,d\dot{y}_i \tag{73}$$

Temporarily drop the subscripts i for convenience and assume that the patch of turbulence is completely Gaussian. In this case the joint probability expression will be:

$$p(y,\dot{y}) = \frac{1}{2\pi\sigma_y\sigma_{\dot{y}}}\, e^{\frac{-y^2}{2\sigma_y^2}}\, e^{\frac{-\dot{y}^2}{2\sigma_{\dot{y}}^2}} \tag{74}$$

Combine the two foregoing equations and consider only one type of turbulence:

$$N = P \int_0^\infty \frac{\dot{y}}{2\pi\sigma_y \sigma_{\dot{y}}} e^{\frac{-\dot{y}^2}{2\sigma_{\dot{y}}^2}} e^{\frac{-y^2}{2\sigma_{\dot{y}}^2}} d\dot{y} \tag{75}$$

Moving the constants outside of the integral sign gives:

$$N = \frac{P}{2\pi\sigma_y \sigma_{\dot{y}}} e^{\frac{-y^2}{2\sigma_y^2}} \int_0^\infty \dot{y}\, e^{\frac{-y^2}{2\sigma_{\dot{y}}^2}} d\dot{y} \tag{76}$$

In order to evaluate the integral, make the following temporary substitutions:

$$y^2 = u^2 \tag{77}$$

and

$$\frac{-1}{2\sigma_{\dot{y}}^2} = c \tag{78}$$

then

$$\int_0^\infty \dot{y}\, e^{\frac{-y^2}{2\sigma_{\dot{y}}^2}} dy = \int_0^\infty u\, e^{-cu^2} du \tag{79}$$

$$= \frac{-1}{2c} e^{-cu^2} \Big]_0^\infty = \frac{1}{2c} \tag{80}$$

Substituting the original expression for c gives:

$$\int_0^\infty \dot{y}\, e^{\frac{-\dot{y}^2}{2\sigma_{\dot{y}}^2}}\, d\dot{y} = -\sigma_{\dot{y}}^2 \tag{81}$$

hence

$$N = \frac{P}{2\pi}\left(\frac{-\sigma_{\dot{y}}}{\sigma_y}\right) e^{\frac{-y^2}{2\sigma_y^2}} \tag{82}$$

Now consider the power spectrum of the response of the design parameter. The area under the power spectrum is the mean square value:

$$\sigma_y^2 = \int_0^\infty \phi(\omega)\, d\omega \tag{83}$$

Assuming that the process is random and stationary, the expected value of the velocity at a particular frequency ω is given by:

$$\dot{y} = i\omega y \tag{84}$$

Hence, the power spectrum of the velocity is given by:

$$\phi_y(\omega) = -\omega^2\, \phi_y(\omega) \tag{85}$$

Therefore, the mean square value of $\dot{y}$ in terms of the power spectrum of y is:

$$\sigma_{\dot{y}}^2 = -\int_0^\infty \omega^2\, \phi_y(\omega)\, d\omega \tag{86}$$

hence

$$\frac{\sigma_{\dot{y}}}{\sigma_y} = -\sqrt{\frac{\int_0^\infty \omega^2\, \phi_y(\omega)\, d\omega}{\int_0^\infty \phi_y(\omega)\, d\omega}} \tag{87}$$

Substituting this result into the foregoing expression for the number of exceedances of level y gives:

$$N(y) = P\, N_0\, e^{\frac{-y^2}{2\sigma_y^2}} \tag{88}$$

where

$$N_0 = \sqrt{\frac{\int_0^\infty \omega^2 \phi_y(\omega)\, d\omega}{\int_0^\infty \phi_y(\omega)\, d\omega}} \tag{89}$$

The above expression is the desired result for flight through a single patch of stationary Gaussian turbulence where the rms value of the response is σ_y.

Now assume that the aircraft flies through a number of such patches, where each patch has an rms response selected at random from a distribution with a probability density $q(\sigma_y)$. The number of exceedances of the level y per unit time will be:

$$N(y) = P\, N_0 \int_0^\infty q\,(\sigma_y)\, e^{\frac{-y^2}{2\sigma_y^2}}\, d\sigma_y \tag{90}$$

Assume that $q(\sigma_y)$ is a Gaussian distribution that is restricted to positive values of the random variable, and therefore the amplitude has been appropriately multiplied by 2:

$$q(\sigma_y) = \sqrt{\frac{2}{\pi}}\, \frac{1}{\sigma}\, e^{\frac{-\sigma_y^2}{2\sigma^2}} \tag{91}$$

where

σ = rms value of design parameter taken over all patches of turbulence

Combining the two foregoing equations gives:

$$N(y) = \frac{P\,N_0}{\sigma}\sqrt{\frac{2}{\pi}} \int_0^\infty e^{\frac{-\sigma_y^2}{2\sigma^2}}\, e^{\frac{-y^2}{2\sigma_y^2}}\, d\sigma_y \tag{92}$$

From MATHEMATICAL TABLES FROM HANDBOOK OF CHEMISTRY AND PHYSICS, Tenth Edition, page 275, Integral #427:

$$\int_0^\infty e^{\left(-x^2 - a^2/x^2\right)}\, dx = \frac{\sqrt{\pi}\, e^{-2a}}{2} \tag{93}$$

Let

$$x^2 = \frac{\sigma_y^2}{2\sigma^2} \tag{94}$$

and

$$\frac{a^2}{x^2} = \frac{y^2}{2\sigma_y^2} \tag{95}$$

Then

$$dx = \frac{d\sigma_y}{\sqrt{2}\,\sigma} \tag{96}$$

and

$$a = \frac{y}{2\sigma} \tag{97}$$

Substituting into the foregoing integral gives:

$$\int_0^\infty e^{\left(-\frac{\sigma_y^2}{2\sigma^2} - \frac{y^2}{2\sigma_y^2}\right)} \frac{d\sigma_y}{\sqrt{2}\,\sigma} = \frac{\sqrt{\pi}}{2}\, e^{-\frac{y}{\sigma}} \tag{98}$$

or

$$\int_0^\infty e^{-\frac{\sigma_y^2}{2\sigma^2}} \, e^{\frac{-y^2}{2\sigma_y^2}} \, d\sigma_y = \sigma \sqrt{\frac{\pi}{2}} \, e^{\frac{-y}{\sigma}} \tag{99}$$

Substituting this result into the previous expression for N(y) gives:

$$N(y) = P \, N_o \, e^{\frac{-y}{\sigma}} \tag{100}$$

The subscripts i were dropped for convenience and they are reinstated now:

$$N(y) = N_o \sum_i P_i \, e^{\frac{-y}{\sigma_i}} \tag{101}$$

Recalling that:

$$\sigma_i = \bar{A} \, b_i \tag{102}$$

gives

$$N(y) = N_o \sum_i P_i \, e^{\frac{-y}{\bar{A} b_i}} \tag{103}$$

which for i = 1, 2 gives the desired result.

$$N(y) = N_o \left\{ P_1 \, e^{\frac{-y}{\bar{A} b_1}} + P_2 \, e^{\frac{-y}{\bar{A} b_2}} \right\} \tag{104}$$

APPENDIX B
SELF-SIMILARITY RELATION FOR VON KARMAN SPECTRA

This appendix demonstrates that the existence of the inertial subrange of atmospheric turbulence implies that the wavelength λ and the amplitude h are related in a statistical sense by:

$$h \propto \lambda^{1/3} \tag{105}$$

Consider the von Karman representation for the power spectra of the atmosphere:

$$\phi(\Omega) = \frac{\sigma^2 L}{\pi} \frac{1 + \frac{8}{3}(1.339 L \Omega)^2}{\left[1 + (1.339 L \Omega)^2\right]^{11/6}} \tag{106}$$

The inertial subrange is that part of the power spectrum which displays a constant -5/3 slope. This occurs for large values of Ω:

$$\lim_{\Omega \to \infty} \left(\frac{\phi(\Omega)}{\sigma^2}\right) \propto \Omega^{-5/3} \tag{107}$$

On a log-log plot of $\phi(\Omega)/\sigma^2$ vs Ω, the slope is -5/3:

$$\text{Log} \lim_{\Omega \to \infty} \left(\frac{\phi(\Omega)}{\sigma^2}\right) \propto -\frac{5}{3} \text{Log}(\Omega) \tag{108}$$

The power spectral density function may be defined by:

$$\phi(\Omega) = \lim_{\substack{\Delta\Omega \to 0 \\ T \to \infty}} \frac{1}{\Delta\Omega T} \int_0^T h(\Delta\Omega, \Omega, t)\, dt \tag{109}$$

or

$$\frac{\phi(\Omega)}{\sigma^2} \propto \frac{h^2}{\Delta\Omega} \tag{110}$$

Assume that:

$$h \propto \Omega^{\gamma} \tag{111}$$

then

$$\frac{\phi(\Omega)}{\sigma^2} \propto \frac{\Omega^{2\gamma}}{\Delta\Omega} \propto \Omega^{2\gamma-1} \tag{112}$$

But

$$\frac{\phi(\Omega)}{\sigma^2} \propto \Omega^{-5/3} \tag{113}$$

Therefore

$$\Omega^{2\gamma-1} \propto \Omega^{-5/3} \tag{114}$$

hence

$$\gamma = -\frac{1}{3} \tag{115}$$

Substituting into Equation 111 gives:

$$h \propto \Omega^{-\frac{1}{3}} \tag{116}$$

Frequency and wavelength are inversely related. Therefore:

$$h \propto \lambda^{\frac{1}{3}} \tag{117}$$

Equation 117 is the desired result.

REFERENCES

1. R. S. Scorer, "The Mechanics of Clear Air Turbulence," A paper prepared for the International Conference on Atmosphere Turbulence, 18-21 May 1971.

2. R. H. Rhyne and Roy Steiner, Power Spectral Measurement of Atmosphere Turbulence In Severe Storms and Cumulus Clouds, NASA TN D-2649, Langley Research Center, October 1964.

3. J. C. Houbolt, Roy Steiner, and K. G. Pratt, Dynamic Response of Airplanes to Atmospheric Turbulence Including Flight Data on Input and Response, NACA TR R-199, Langley Research Center, June 1964.

4. F. M. Hoblit, Neil Paul, J. D. Shelton, and F. E. Ashford, Development of a Phone-Spectral Gust Design Procedure for Civil Aircraft, FAA-ASD-53, The Federal Aviation Agency, January 1966.

5. W. P. Rodden, J. P. Giesing, and T. P. Kalman, "New Developments and Applications of the Subsonic Doublet - Lattice Method for Non-planar Configurations," AGARD Symposium on Unsteady Aerodynamic Analysis of Interfering Surfaces," AGARD-CP-80-71 Paper No. 4, November 1970.

6. Bernard Etkin, Dynamics of Atmosphere Flight, Wiley Press, 1972.

7. J. R. Fuller, L. D. Richmond, C. D. Larkins and S. W. Russell, Contributions to the Development of a Power Spectral Gust Design Procedure for Civil Aircraft, Aircraft Development Service, Federal Aviation Agency, July 1965.

8. J. S. Bendat and A. G. Piersol, Measurement and Analysis of Random Data, Wiley Press, 1956.

9. R. A. Cox, "A Comparative Study of Aircraft Gust Analysis Procedures," The Aeronautical Journal of the Royal Aeronautical Society, Vol. 74, Pages 807-813, October 1970.

10. Military Specification, Airplane Strength and Rigidity, Flight Loads, MIL-A-008861A(USAF), 31 March 1971.

11. J. C. Houbolt, Gust Design Procedures Based on Power Spectral Techniques, AFFDL-TR-67-74, Air Force Flight Dynamics Laboratory, Air Force Systems Command, WPAFB, August 1967.

12. F. E. Pritchard, C. C. Easterbrook, and G. E. McVehil, Spectral and Exceedance Probability Models of Atmospheric Turbulence for Use in Aircraft Design and Operation, AFFDL-TR-65-122, Air Force Flight Dynamics Laboratory, Air Force Systems Command, WPAFB, November 1965.

REFERENCES (CONTINUED)

13. L. J. Howell and Y. K. Lin, "Response of Flight Vehicles to Nonstationary Atmospheric Turbulence," AIAA Journal, Vol. 9, No. 11, November 1971.

14. P. M. Reeves, R. G. Joppa, and V. M. Ganzer, A Non-Gaussian Model of Continuous Atmosphere Turbulence for Use in Aircraft Design, NASA CR-2639, National Aeronautics and Space Administration, January 1976.

15. M. B. Priestly, "Power Spectral Analysis of Non-Stationary Random Processes," Journal of Sound and Vibration, Vol. 6-I, Pages 86-97, 1967.

16. W. D. Mark and R. W. Fischer, Investigation of the Effects of Nonhomogeneous Behavior on the Spectra of Atmospheric Turbulence, Report No. 3233, Bolt Beranek and Newman Inc., February 1976.

17. J. A. Dutton and D. G. Deaven, "A Self-Similar View of Atmospheric Turbulence" International Symposium on Spectra of Meteorological Variables, Session 3b, Stockholm, Sweden, 9-19 June 1969.

18. J. C. Houbolt, Preliminary Development of Gust Design Procedures Based on Power Spectral Techniques, AFFDL-TR-66-58, Vols. 1 and 2, Air Force Flight Dynamics Laboratory, Air Force Systems Command, WPAFB, July 1966.

19. W. H. Austin, A Summary of Some Recent Developments in the Description of Atmospheric Turbulence Used for Aircraft Structural Design, SEG-TR-66-45, Systems Engineering Group, Air Force Systems Command, WPAFB, August 1966.

20. J. W. McCloskey, J. K. Luers, J. P. Ryan, and N. A. Engler, Statistical Analysis of Lo-Locat Turbulence Data for Use in the Development of Revised Gust Criteria, AFFDL-TR-71-29, Air Force Flight Dynamics Laboratory, Air Force Systems Command, WPAFB, April 1971.

☆U.S.Government Printing Office: 1977 — 757-001/101